UILU-ENG-73-2002

CIVIL ENGINEERING STUDIES
STRUCTURAL RESEARCH SERIES NO. 395
Illinois Cooperative Highway Research Program
Series No. 137

THE EFFECT OF INTERNAL WELD DEFECTS ON THE FATIGUE BEHAVIOR OF WELDED CONNECTIONS

By
DAVID H. EKSTROM
W. H. MUNSE

Report on Phase 2.3
Investigation of Welded Highway Bridges
Project IHR-64

Conducted in
THE STRUCTURAL RESEARCH LABORATORY
DEPARTMENT OF CIVIL ENGINEERING
ENGINEERING EXPERIMENT STATION
UNIVERSITY OF ILLINOIS AT URBANA-CHAMPAIGN
in cooperation with
THE STATE OF ILLINOIS
DEPARTMENT OF TRANSPORTATION
DIVISION OF HIGHWAYS
and
THE U.S. DEPARTMENT OF TRANSPORTATION
FEDERAL HIGHWAY ADMINISTRATION

UNIVERSITY OF ILLINOIS
URBANA, ILLINOIS

FEBRUARY 1973

TECHNICAL REPORT STANDARD TITLE PAGE

1. Report No.	2. Government Accession No.	3. Recipient's Catalog No.
UILU-ENG-73-2002		

4. Title and Subtitle	5. Report Date
The Effect of Internal Weld Defects on the Fatigue Behavior of Welded Connections	February 1973
	6. Performing Organization Code

7. Author(s)	8. Performing Organization Report No.
David H. Ekstrom and W. H. Munse	SRS 395 ICHRP No. 137

9. Performing Organization Name and Address	10. Work Unit No.
Department of Civil Engineering University of Illinois Urbana, Illinois 61801	11. Contract or Grant No. IHR-64
	13. Type of Report and Period Covered Final Technical Report
12. Sponsoring Agency Name and Address The State of Illinois Department of Transportation Division of Highways Springfield, Illinois 62706	14. Sponsoring Agency Code

15. Supplementary Notes

Prepared in cooperation also with the U.S. Department of Transportation, Federal Highway Administration

16. Abstract

The object of this investigation was to study the effect of internal flaws on the fatigue behavior of butt-welded connections in mild structural steel, the initiation of fatigue cracks from these flaws and the propagation rates of these cracks in the connections. Since internal flaws occur in many welds it is essential to obtain a better understanding of the behavior of flawed connections so that adequate, yet realistic, code requirements can be established.

The study is limited to two major types of defects, porosity and incomplete penetration. The porosity was further subdivided into two categories based on the severity of the defect. The specimens with incomplete penetration were made with an initial 3/16" centrally located crack the full width of the specimen.

The fatigue behavior of the connections with the defects is compared with that of sound welds to observe the effects of the defects on the fatigue strength of the connections. The data are compared with results of similar studies found in the literature and also with the AASHO 1970 Specification design requirements.

Three of the specimens with incomplete penetration were examined radiographically during the fatigue testing to determine when initiation of the fatigue cracks occurred, and how rapidly they propagated. The results of the crack propagation tests are compared with similar relationships developed for high strength steels. A relationship that better fits the data for mild steel has been developed in a manner similar to that used for the high strength steels.

17. Key Words	18. Distribution Statement
Fatigue, welds, connections, weld defects, porosity, lack of penetration, crack propagation, crack initiation, AASHO specification, ASTM-A36 steel	

19. Security Classif. (of this report)	20. Security Classif. (of this page)	21. No. of Pages	22. Price
Unclassified	Unclassified	90	

Form DOT F 1700.7 (8-69)

DISCLAIMER

The contents of this report reflect the views of the authors who are responsible for the facts and the accuracy of the data presented herein. The contents do not necessarily reflect the official views or policies of the Illinois Department of Transportation or the Federal Highway Administration. This report does not constitute a standard, specification, or regulation.

TABLE OF CONTENTS

LIST OF TABLES

LIST OF FIGURES

1. Introduction

Discontinuities, such as lack of penetration, lack of fusion, shrinkage cracks, slag inclusions, and porosity are found in many welded connections. The presence of such discontinuities in a connection, if they are of sufficient magnitude, can be expected to lower the strength of a connection, especially when it is subject to cyclic loading. Some of the current fatigue specifications[1] place limits on the degree of defect allowed in a weld, but do not differentiate between type of steel or type of defect, or relate the degree of defect to the expected behavior of the connection. To insure that these design specifications are adequate and at the same time realistic for the design of such structures as bridges it is necessary to better understand the manner in which weld flaws or discontinuities affect the fatigue behavior of welded members or connections.

The principal highway bridge design and fabrication specifications[1,2] are based on limited amounts of data on mild steel connections with defects. Some of these fatigue tests on welds with defects are reported in the literature;[3,4,5] however, they have not been of sufficient scope or number to permit a quantitative evaluation of the effect of the defects.

An earlier portion of this program was concerned with the predictions of the fatigue life of a connection fabricated with a lack of penetration.[6] By using photoelastic models of the flaws to determine the associated stress fields at the tips of the flaws, a correlation was

obtained between the fatigue life, the flaw shape, and the material properties. However, a much more complete evaluation and many more actual test results are necessary to properly evaluate the energy criteria proposed in the study. Furthermore, a better definition of the effect of weld quality with respect to material properties would aid in establishing better and more realistic specification requirements for weld quality.

Two other important aspects of fatigue behavior of welded connections that should be taken into account in the development of design specifications are the initiation and the propagation of fatigue cracks from weld flaws. Information relating flaw or crack size and the applied stresses to these two parameters would be most helpful in establishing inspection and repair requirements and procedures. There are a number of recent reports concerned with the question of crack propagation in steels, but relatively little information on their relationship to welds and weld flaws. Part of the study reported herein has been conducted, therefore, to assist in providing some of the required data discussed above.

2. Object and Scope of Investigation

The present study examines the effects of internal flaws on the fatigue behavior of butt-welded connections in a mild structural steel, the initiation of fatigue cracks from the flaws, and the rate of propagation of these cracks.

Results of these tests and other tests reported in the literature are compared to indicate the effect the internal flaws had on

the fatigue behavior of the connections. However, the study has been limited to two major types of defects, porosity in varying degrees, and incomplete penetration.

Prior to fabrication of the test specimens a study was conducted to establish welding procedures that would consistently produce the desired flaws in the welds. Procedures were required that would make it possible to control the size and distribution of the flaws from one specimen to the next and thus permit the preparation of test specimens of a given weld quality.

In addition to the evaluation of the fatigue resistance of weldments with flaws, data has been gathered in some of the tests to determine the rate of fatigue crack propagation from the flaws. To study crack propagation the specimens were radiographed periodically during the tests and the time of fatigue crack initiation and rate of crack propagation determined by observing and measuring the flaw size on the radiographs.

The defects that were studied were intended to simulate those that might exist in actual structures. It is hoped, therefore, that the observations made during these tests might make possible the establishment of better and more realistic inspection and design requirements.

A detailed description of the investigation is given in the following sections. A summary of the materials and specimens is presented in Sections 3, a description of the testing equipment is given in section 4, and a discussion of the fatigue behavior study and crack propagation study are presented in sections 5 and 6, while a detailed

discussion of the preliminary welding procedure study is presented in Appendix A.

3. Description of Materials and Specimens

3.1 Materials

The fatigue specimens were fabricated from a steel conforming to ASTM Specification A36. The physical properties and chemical composition of the steel, as given in the mill report, are as follows:

1. Physical Properties

   Yield Pt. 41,100 psi, Ult. Tensile Strength 70,900 psi, Elongation 27% (in 8 in.)

2. Chemical Composition

   C = 0.23%; Mn = 0.9%; P = 0.015%; S = 0.030%

The welding electrode used was a 1/16" ϕ wire equivalent to E70 grade electrodes with a minimum ultimate tensile strength of 70,000 psi (AWS Spec. A5.1-58T and ASTM Spec. A233-58T). The typical chemical composition of the weld metal as given by the manufacturer is as follows:

3. Chemical Composition

   C = 0.09%; Mn = 1.00%; P = 0.017%; S = 0.024%

   Si = 0.45%

The steel plate used for the test specimens was 3/4-in. thick. A 36-in. long groove weld was prepared in the plate and the individual specimens were then cut from the weldment and machined to a test section width of 1-1/2in.(see Fig. 3.1). The 3/4 x 1-1/2 in. cross-section

dimensions were chosen mainly for purposes of radiography. To examine crack propagation rates in some of the specimens radiographs had to be taken through the width of the specimen(along the crack). Radiography through large thicknesses of material becomes more difficult and time consuming so the specimen width was limited to the 1-1/2 in. dimension. Limiting the dimensions to 3/4 in. x 1-1/2 in. also decreased the loads necessary for testing to such a level that the University's 50,000 lb capacity fatigue testing machines could be used. These machines operate at a speed of 300 cycles per minute and reduce to a minimum the amount of time necessary for testing.

3.2 Welding Procedure

Specimens were made with

1. Sound welds
2. Porosity equivalent approximately to the limit permitted by the AWS Specifications for weldments containing defects
3. Severe clusters of porosity in the weldment
4. Welds containing a lack of penetration of approximately 3/16 in.

Figures 3.2(a) and (b) are prints of radiographs of specimens showing the two degrees of porosity studied.

Since the principal variable to be examined was the effect of the weld flaws, it was necessary to reduce to a minimum other variables that might enter into the testing and affect the results. To achieve

this condition automatic gas-metal arc welding was used to eliminate the human element from the welding. Prior to actually welding the specimens a preliminary study of welding procedures was conducted to determine the parameters that would produce sound welds and the changes in these parameters that would produce the desired defects. In addition, the welding procedure for the sound welds was qualified in accordance with the requirements of the AWS Specifications.[1] The qualification testing consisted of two reduced section tension tests, two root bend tests, and two face bend tests. After satisfactory qualification of the procedure, the various welding parameters, such as voltage, current, type of shielding gas, shielding gas flow, etc., were changed to obtain the desired defects. A detailed description of the parameter changes tried and their effect on the welds appears in Appendix A. The following is a summary of the welding procedures that gave reproducable defects and were used in fabricating the test specimens.

Welding Procedures

1. Sound Weld Specimens S1-1 to S1-5

V-Groove (Figure 3.3a)

1st Pass--28V., 320 AMPS., TRAVEL SPEED 12 I.P.M.
2nd Pass--28V., 330 AMPS., TRAVEL SPEED 12 I.P.M.
3rd-6th Pass--28V., 320 AMPS., TRAVEL SPEED 12 I.P.M.
Shielding gas was 95% Argon--5% oxygen mixture, at a flow rate of 50 CFH.
First pass was back ground.
Oscillator was used for all passes.

2. Porosity--AWS Specification Allowable Specimens PC4-1 to PC4-4

V-Groove (Figure 3.3a)

1st Pass--28V., 320 AMPS., TRAVEL SPEED 12 I.P.M.
2nd Pass--25V., 330 AMPS., TRAVEL SPEED 12 I.P.M.
(Voltage reduced to produce porosity)*
3rd-6th Pass--28V., 320 AMPS., TRAVEL SPEED 12 I.P.M.
Shielding gas was 95% Argon--5% oxygen mixture, at a flow rate of 50 CFH.
First pass was back ground.
Oscillator was used in all passes.

3. Porosity--Severe Specimens PS5-1 to PS5-5

V-Groove (Figure 3.3a)

1st Pass--28V., 320 AMPS., TRAVEL SPEED 12 I.P.M.
2nd Pass--28V., 330 AMPS., TRAVEL SPEED 12 I.P.M.
(To introduce pore clusters, the gas flow was interrupted for periods of one second at the desired location of defects.)*
3rd -6th Pass--28V., 320 AMPS., TRAVEL SPEED 12 I.P.M.
Shielding gas was 95% Argon--5% oxygen mixture, at a flow rate of 50 CFH.
First pass was back ground.
Oscillator was used in all passes.

4. Lack of Penetration--3/16-in.--Type I Specimens LP1-2-1 to LP1-2-5

U-Groove (Figure 3.3b)

1st and 2nd Pass--28V., 300 AMPS., TRAVEL SPEED 12 I.P.M.
3rd-6th Pass--28V., 300 AMPS., TRAVEL SPEED 12 I.P.M.
Shielding gas was 95% Argon--5% oxygen mixture, at a flow rate of 50 CFH.
Oscillator was used in all passes.

5. Sound Weld Specimens LP2-3-1 to LP2-3-5

U-Groove (Figure 3.3c)

1st and 2nd Pass--28V., 300-320 AMPS., TRAVEL SPEED 12 I.P.M.
3rd-6th Pass--28V., 310 AMPS., TRAVEL SPEED 10 I.P.M.
Shielding gas was 95% Argon--5% oxygen mixture, at a flow rate of 50 CFH.
Oscillator was used in all passes.

---

* The porosity was placed in the second weld pass to locate the defects at approximately midthickness of the specimen.

6. Lack of Penetration--3/16-in.--Type I Specimens LP2-6-6 to LP2-6-10

U-Groove (Figure 3.3b)

1st and 2nd Pass--28V., 270-310 AMPS., TRAVEL SPEED 12 I.P.M.
3rd-6th Pass--28V., 290-310 AMPS., TRAVEL SPEED 10 I.P.M.
Shielding gas was 95% Argon--5% oxygen, at a flow rate of 50 CFH.
Oscillator used in all passes.

The oscillator referred to in these procedures is a device that was attached to the welding carriage and caused the arc to move from side to side across the groove. Its purpose was to give a flatter weld bead, better fusion with the side of the groove, and to prevent the arc from burning too deeply into the base metal at the center of the groove. The preheat and interpass temperatures for all of the welding was 150° F.

Originally a series of test specimens containing a lack of penetration of 1/16-in. was planned but, in welding the specimens, complete penetration was obtained. These specimens were welded with procedure listed as number 5 but were tested as sound welded joints since the penetration was complete and no defects were visible. The procedure was then modified as noted in procedure 6 and another set of specimens was welded. This time the lack of penetration was found to be approximately 3/16-in. so the specimens were grouped with the lack of penetration type-I specimens.

3.3 Specimen Fabrication

The steel was cut into pieces 36-in. long by 16-in. wide as shown in Figure 3.4. These pieces were then grooved in accordance with the dimensions given in Figure 3.3.

The saw-cut edges of the plates for the V-grooves were milled to the dimensions in Figure 3.3. However, the specimens with the U-groove (for the lack of penetration) were designed to have a zero root gap. Consequently, the two edges to be welded were machined smooth, the two plates were butted together and then tack welded to hold the pieces in position. The groove was then machined in accordance with Figure 3.3.

Six weld passes were used to weld the plates with alternate passes being placed on opposite sides of the plate as shown in Figure 3.5 and in a direction opposite that of the previous pass. The first weld pass in the V-groove specimens was background to sound weld metal to insure adequate penetration of the second pass along the entire length of the weld.

After the plates had been welded they were radiographed to determine what defects if any were present in the weld and where they were located. The specimens with the desired degree of porosity were positioned from these radiographs and then cut as shown in Figure 3.6.

The lack of penetration was not visible on the radiographs but, even if it had been, it would have been impossible to measure its depth from the radiograph. As a result, the 36-in. long plates with incomplete penetration were cut into five pieces of equal width which were then machined as shown in Figure 3.7. One piece adjacent to the fatigue specimen was bent to open up the crack (lack of penetration) and another piece was polished and etched to show the weld and lack of penetration. The approximate size of flaw was determined by measuring the opened crack of the bend specimen or the unpenetrated section of the base metal on the polished and etched specimen (see Figure 3.8).

Prior to fatigue testing the weld reinforcement was removed and the surfaces of the specimens in the test section were polished with a belt sander. The purpose of the polishing was to remove any additional stress raisers that might result from milling marks or scratches and cause the specimen to fail at a location other than the intended defect (see Figure 3.9).

4. Description of Testing Equipment

4.1 Fatigue Testing Machines

The fatigue machines used for the tests reported herein were the University of Illinois' 50,000 lb capacity lever type fatigue testing machines. A photograph and schematic diagram of the machines is shown in Figure 4.1. These machines operate at a frequency of approximately 300 load cycles per minute.

The load was measured by means of proving-ring type dynamometers in three of the four machines while in the fourth it was measured using a strain-gage weighbar. The dynamometers and the weighbar were wired with electrical resistance strain gages. By reading the strains from strain indicators and knowing the calibration constants for the fatigue machines the load on the specimens could be determined. Prior to the initiation of testing, each of the machines was recalibrated. In addition to load measurement by means of the strain gage system, the load on the specimens in the three machines with the dynamometers was checked by using dial gages to measure the deformation of the dynamometer. Figure 4.2 shows the various devices for load indication.

4.2 Radiographic Equipment

Two groups of radiographs were obtained in the investigation. During the fabrication of the test specimens radiographs were obtained using a 300 KV-6MA X-ray unit and standard x-ray inspection techniques and procedures to obtain an indication and record of the initial quality of the welds in the specimens. These records were used also to select the positions at which the individual test specimens were to be located.

The second group of radiographs to be taken were those used to determine the time of crack initiation and the rate of crack propagation in the fatigue tests. These radiographs were taken with a 200 KV-5MA X-ray unit. Figure 4.3 shows the unit as it was set to radiograph specimens in the fatigue machines. The crack propagation radiographs were taken when the test specimens were under maximum tensile loading.

5. Description of Fatigue Tests and Analysis of Results

5.1 Description of Tests

The fatigue test program consisted of testing the four types of specimens described in section 3 under cyclic loading. The values of stress applied to the specimens were varied to yield fatigue lives that were of both long and short duration so that S-N curves could be determined. Table 5.1 is a summary listing of the tests that were conducted in the program. It presents the type of defects tested, the expected life range of the specimens and the number of specimens tested in each category.

The first series of ten specimens contained sound welds so that there would be a basis for comparison between the fatigue behavior of sound welds and welds containing flaws.

The second series of four specimens contained welds in which small amounts of porosity had been deposited. The amount of porosity in the weld was approximately that allowed by the AWS Specifications for railway and highway bridge design.[1] These specifications limit the size of defect in the weld, the spacing between the defects and sum of the defect dimensions in a specified length of weld. The four specimens fabricated for the "AWS-allowable" series of tests were intended to show the behavior of connections designed and fabricated in compliance with present specifications.

Another series of five tests was conducted on specimens containing large clusters of porosity centrally located in the weld. This type of defect could occur in a weld produced by the gas-shielded metal arc welding process if the gas flow was momentarily interrupted, and is precisely the manner in which the defect was produced for the test specimens. For a given structure, unless the specified inspection procedure calls for checking of the entire length of a weld, such defects could go undetected and uncorrected. Thus, this third series of tests makes possible a comparison of the fatigue behavior of connections with this severe defect and connections that are within the AWS specification requirements.

Finally, a series of ten specimens containing a lack of penetration at midthickness was tested. The placing of a lack of

penetration in the weld is similar to placing a small crack at mid-thickness of the specimen through the full width of the specimen. The depth of the lack of penetration (the dimension in the thickness direction) was approximately 3/16-in. in all specimens tested.

It is extremely difficult to detect the lack of penetration by nondestructive testing because the crack is closed tightly as a result of the weld shrinkage. Attempts to locate and measure the crack, both radiographically and with ultrasonic equipment, were unsuccessful. Consequently, the defect size prior to testing was determined by examining the pieces cut from the sides of the fatigue test specimen as described in Section 3. Because of the difficulty encountered in measuring nondestructively the lack of penetration, it is conceivable that this type of defect could easily go undetected under normal inspection procedures.

In order to obtain information regarding the effects of the defects on the fatigue behavior of the connections it was necessary to have all failures initiate at the defects, and to eliminate any effects of the joint surface on this behavior. This required that all of the welds have the reinforcement machined off and the surfaces polished.

To obtain test results for both long and short lives, variations were introduced in the stresses and stress ratios used in the tests. These variations were necessitated also by the desire to obtain short lives with the sound welded connections without exceeding the yield point of the steel. To do this with a minimum number of variables it was decided to test all specimens at a maximum gross area stress of 36 ksi (somewhat below the base metal yield point of 41.1 ksi) and to vary the stress

range and stress ratio to obtain the short and long life tests. In spite of this limitation on maximum stress it appeared that yielding did occur in the weld metal of some of the specimens containing large defects. In the early stages of testing the load on some specimens had to be reset frequently to keep the maximum stress up to 36 ksi, although the yield strength of the weld metal was determined to be approximately 52 ksi. Thus, the net section stresses on some of the specimens, because of the flaw size, must have been slightly in excess of 52 ksi.

After the specimens were placed in the fatigue machines and the fatigue loads properly adjusted, the members were radiographed prior to the start of the fatigue tests. In the case of the lack of penetration specimens the radiographs were taken with the maximum load applied to the specimen in an effort to open the flaw to a maximum for the radiograph. Generally, this flaw type was not visible on the initial radiographs. The specimens with all other defect types were radiographed under zero load. These radiographs provided a record of the initial condition of the connection and a basis on which to relate the weld quality to the design specifications.

After the specimens had been radiographed the machines were started and the tests run to specimen failure or until it was decided they would not fail under the stress cycle at which they were being tested. Periodically during the tests the machines were stopped so that the load could be checked and reset if necessary, and to radiograph specimens being used to study crack propagation.

Failure of the specimen was taken as the number of cycles at which the crack had progressed sufficiently to trip a limit switch attached to the pull heads of the machine, thereby shutting the machine off. At this point the specimen would no longer carry the initial load and the number of additional cycles to complete rupture was insignificant with respect to the total life.

5.2 Results of Fatigue Tests

The data from the fatigue tests are presented in Table 5.2 and summarized in Table 5.3. Figures 5.1 to 5.5 are graphical representations of the data in terms of S-N curves and make possible comparison of the effects of the various defects. The fatigue strength at 100,000 cycles and 2,000,000 cycles was computed using a least squares best fit. Limits of two standard deviations are also presented on the S-N curves.

A summary comparison of the fatigue test results of the different types of defects studied in this program is presented in Figure 5.5. In this comparison, as well as the presentation of Figure 5.1, the data from welds with porosity within the limits of the AWS specification[1] requirements have been combined with the data from sound welds. It is evident, particularily in Figure 5.5, that the fatigue resistance of the connections was markedly affected by the severe internal weld flaws.

Comparisons are possible also with data reported in the literature for similar tests.[3,4] Figures 5.6 and 5.7 show how the test

results of the present study compare to others found in the literature. Here again it is evident that the weld flaws can have a significant effect on the fatigue resistance of the members.

A further comparison of the fatigue data can be made with the allowable stress provisions of the design specifications. Such a comparison is made in Figure 5.8 which is a modified Goodman diagram showing how the test results relate to the requirements of the 1971 AASHO design specifications.[2]

5.3 Discussion and Analysis of Test Results

The specimens listed in Table 5.2 marked with (+) are those which had not failed at the lives and stresses given in the table. They were allowed to run for between 5 to 10 million cycles at which point the stress was increased and the specimens then run to failure. For the purposes of computing and plotting the S-N curves the lives of those specimen which had not failed were taken as 2 million cycles. The data obtained in the retest of these specimens were not used to establish the S-N curves because the fatigue resistance may have been affected by the earlier loading history. However, the data from these specimens have been plotted on the curves (Figures 5.1, 5.2, and 5.3). In the case of specimens S1-1B and S1-3A, the understressing does not appear to have affected the fatigue resistance of the members. However, the fatigue resistance of specimen LP2-6-9A appears to have been improved considerably by the understressing.

The specimens fabricated with sound welds were machined and polished to remove the surface stress raisers. As a result their fatigue

resistance was relatively high. In addition, a relatively small scatter band, as shown in Figure 5.1, was obtained. However, this is misleading because the S-N curve for this type of member is extremely flat and the variation in life at a given stress can be relatively large. An examination of the data in Table 5.2 indicates just how large this range in lives is. Specimens S1-3 and LP2-3-4 were both subjected to a stress range of 40 ksi, and had lives of 10,953,000 cycles (without failure) and 275,700 cycles, respectively. Nevertheless, these data and the associated S-N curve provide a good basis for determining the effects of various defects on the fatigue resistance of the connections.

Relatively little conclusive information was obtained from the connections with porosity within the requirements of the AWS Specification[1] because two of the specimens (those tested at the higher stress ranges) broke outside of the weld and a third specimen ran for 5,353,800 cycles. Nevertheless, the data have been plotted in Figure 5.1 along with the data for sound welds. Based on these plots, the following observations can be made:

1. At high stress levels or in the short life region, the small amounts of defects permitted by the Specification did not appear to affect the fatigue resistance of the members to any great extent.
2. The data points do not fall very far from the two standard deviation limits established for the sound welds and can probably be considered to be a part of the same population as the sound welds.

3. At the longer lives, specimens that failed at about 1.5 million and 5.3 million cycles, the data indicate that the fatigue strength was only slightly lower than that of the sound welds due to the presence of the defects.
4. Thus, the fatigue behavior of the connections with porosity within the limitations of the current AWS Specifications[1] appears to be very similar to that of sound welds.

The slope of the S-N curve for the welds with severe clusters of porosity (Figure 5.2) is greater than that for the sound welds and the fatigue strengths at both 100,000 cycles and 2,000,000 cycles are considerably lower. The difference in slope and fatigue strength can readily be observed in Figure 5.5 and on the modified Goodman diagrams of Figure 5.8. Since the defects were of considerable size and generally very irregular in shape two factors were introduced which could have reduced the fatigue lives of the specimens at any given stress range. The first is the irregular shape acting as a notch or stress concentration and the second is the reduction in the cross-sectional area. A combination of these two effects probably contributed to the greatly reduced fatigue resistance of the connections.

The fatigue strengths of the connections with incomplete penetration were even lower than the fatigue strengths of connections containing severe porosity; the slope of the S-N curve is steeper and the amount of scatter in the data is greater (see Figure 5.3).

Even when examined as a function of net-section stress the fatigue resistance of the connections with a lack of penetration was not as great as that of the connections with severe porosity; the lack of penetration apparently produces a weld with extremely poor fatigue strength.

The data obtained from the present study agrees reasonably well with similar data found in the literature[3,4] (see Figures 5.6 and 5.7). Similar trends are evident in the data from all series of specimens containing porosity. The data of the current investigation for sound welds and connections with porosity no greater than that permitted by the AWS Specifications[1] agree very well with the curve established by tests reported for connections with small amounts of porosity. However, the fatigue strength of the connections of the current investigation with severe porosity differed somewhat from that found in the literature for similar connections, but the general pattern of behavior has been similar. This may be due in part to differences in terminology. The definition of "degree of porosity" is vague for some of the data and may be the cause for the shifting of the curves in Figure 5.6.

The lack of penetration examined in the present program was more severe than that reported in the literature for other investigations, however, its fatigue behavior follows the same general pattern as that obtained from connections with lesser amounts of lack of penetration. Thus, as shown in Figure 5.7, the reduction in the fatigue resistance of a member with a lack of penetration increases with the severity of the stress concentrator and also with the life of the members.

All of the data presented herein for various defects tends to converge at the shorter lives (about 30,000 cycles) while at longer lives the effect of the defects increases with an increase in life.

As mentioned previously, there is quite a bit of scatter in the test data. However, the data that were obtained present a general picture of the behavior of defective welds and the following observations relating their fatigue behavior to present specifications can be made.

If the specimens behave as shown by the dotted lines in Figure 5.8 (fatigue resistance is assumed to be a function only of the range of stress--for these members the assumption is believed to be relatively good), the only defect that would cause serious concern if in a connection designed for 2,000,000 cycles according to the AASHO 1971 Specifications[2] would be those with large amounts of lack of penetration. Taking $F_{2,000,000}$ as an example, the AASHO Specification allows a range of 18 ksi with a 20 ksi maximum for a sound butt weld prepared in the general manner in which the specimens of this investigation were prepared. In the test results of this study the only type of defect that has a $F_{2,000,000}$ stress range (average fatigue strength) less than 18 ksi is the lack of penetration with a stress range of 14 ksi. Even the specimens with severe porosity had an average stress range of approximately 25 ksi at 2,000,000 cycles. The specimens with sound welds had a fatigue strength at 2,000,000 cycles of approximately 39.9 ksi. (This is somewhat higher than most data reported in the literature for connections with the reinforcement removed. The reason for this is not known.)

A summary of the fatigue strength of the various types of connections and the ratio of these values to the allowable stress ranges of the current AASHO Specifications[2] are given below.

FATIGUE STRENGTHS OF CONNECTIONS (Stress Range)

Weld Soundness	$F_{100,000}$ ksi	Ratio to Allowable* Stress Range	$F_{500,000}$ ksi	Ratio to Allowable* Stress Range	$F_{2,000,000}$ ksi	Ratio to Allowable* Stress Range
Sound Welds	47.5	1.05	43.2	1.57	39.9	2.22
Severe Porosity	42.3	0.94	32.0	1.16	25.2	1.40
Lack of Penetration	30.4	0.68	20.1	0.73	14.1	0.78

* Allowable stress range in 1971 AASHO Specification for sound butt welds ground flush (45, 27.5 and 18 ksi respectively), but not to exceed +20 ksi. The +20 ksi limit is neglected in determining the above ratios.

Here it may be seen that there is a great lack of consistency in the factor of safety provided by the current specifications, and a very low factor of safety at the shorter lives or when severe porosity or a lack of penetration exists in the connections. It should be borne in mind that the factors of safety shown above are fictitious in that the maximum tensile stress cannot exceed 20 ksi. However, the ratios do give a good indication of the lack of correlation between these test data and the design relationships given in the current Specification.[2]

6. Description of Crack Propagation Study and Analysis of Results

6.1 Introduction to Crack Propagation

The fatigue life of a specimen may be considered to consist of two major stages; the first stage is crack initiation or the time spent in nucleation, and the second stage is that of crack propagation. This latter stage consists of macrocrack growth and final fracture of the specimen.

Studies have recently been conducted by a number of investigators to determine what portion of the fatigue life of a specimen is spent in the crack propagation stage and to correlate the results of the experimental studies with a fracture mechanics analysis.[10-17] However, most of these studies have been conducted on high-strength steels and aluminum alloys. Although the results for the material considered to date appear to be fairly consistent, it is desirable to study also the behavior of mild steel weld metal and to compare these results with the results from the other materials.

6.2 Fracture Mechanics

A fracture mechanics analysis considers the maximum stress or stress intensity that is experienced in the material adjacent to the defect or crack tip. In cyclic loading both the minimum value and the maximum value of stress intensity are important, and in the crack propagation relationships the range of stress intensity is used. In general it has been found that the rate of crack growth can be computed

using the following expression:

$$\frac{da}{dN} = C(\Delta K)^n \tag{1}$$

where:

$\frac{da}{dN}$ = rate of crack growth per cycle

C = material constant

n = material constant

(ΔK) = range of stress intensity factor

Constants C and n depend on the material properties, while (ΔK) is a function of the instantaneous crack dimension and the range of the applied stress.

In a study conducted by Barsom, Imhof, and Rolfe[15] fatigue crack propagation in a number of high strength steels was examined. They found that a conservative estimate of the crack propagation rate could be determined using the following expression:

$$\frac{da}{dN} = 0.66 \times 10^{-8}(\Delta K)^{2.25} \tag{2}$$

All of the data from their tests fell within a band determined from

$$\frac{da}{dN} = C(\Delta K)^{2.25}$$

where the value of C ranged from 0.275×10^{-8} to 0.66×10^{-8}. The values of C and n were determined empirically to fit the experimental data.

For a through crack in a finite plate, as found in the lack of penetration models studied by Radziminski and Lawrence,[10] the following expression was suggested for computing ΔK:

$$\Delta K = \sigma\sqrt{\pi a}\left(\sec\frac{\pi a}{2b}\right)^{1/2} \tag{3}$$

$$0 \leq a \leq 0.8b$$

where:

a = one-half the crack width

b = one-half the plate thickness

σ = the maximum stress for a zero-to-tension stress range

In J. D. Harrison's study[13] ΔK was determined from the expression:

$$\Delta K = \Delta\sigma\sqrt{\pi a}\left(\frac{2b}{\pi a}\tan\frac{\pi a}{2b}\right)^{1/2} \qquad (4)$$

where the variables are all as defined previously. The value of ΔK from this expression is only slightly different from that obtained from expression (3), giving results that are slightly less conservative.

6.3 Crack Propagation Studies

The values for ΔK computed herein are for a crack at mid-thickness and running continuously for the full width of the specimen, as shown in Figure 6.1. For cracks or defects located eccentrically to the centerline of the specimen, the stress intensity range at the point nearest the edge or surface of the member will be greater than if computed for the crack at the centerline and the crack will propagate at a higher rate than computed. Therefore, for an eccentric notch, the half specimen thickness, b, should be taken as the distance from the center of the defect to the nearest surface of the specimen.

The values of C and n are somewhat sensitive to the test environment. The values represented herein are for a room temperature air environment. Knowing values for C and n for the material used and

the environmental conditions along with the defect or initial crack size and the material thickness, the number of cycles to failure can be computed using a numerical integration procedure with Formula 1.

Part of the present study was concerned with determining whether the expressions and constants for predicting the crack propagation life for high strength steels could also be applied to mild steel weld metal and if not, what changes would be necessary to provide the appropriate expression. Three of the fatigue test specimens containing the continuous lack of penetration were examined for crack propagation rates. The severe defect with a large stress range caused short fatigue lives, major portions of which were probably spent in propagation of the crack.

Prior to starting a test each specimen was radiographed perpendicular to the short dimension of the specimen to show the thickness of the specimen and the depth of the crack. The radiographs were taken with the specimen under full load to open the crack up as wide as possible. On this initial radiograph the crack was barely visible, if at all, because the plates were pulled tightly together by the weld. The initial defect size was measured from the bend specimens prior to testing and checked on the fracture surface after failure (see Table 6.1). Thus, upon examination of the radiographs, an approximate measure of the time of initiation and rate of crack propagation could be determined.

All of the crack propagation specimens were run in the latter stages of the fatigue testing program so that the S-N curve established in the earlier tests could be used as a guide in selecting the intervals

between radiographs. The lengths of the intervals between the radiographs and the lengths of the cracks measured on the radiographs are shown in Tables 6.2 to 6.4.

With the radiographic record of the crack size at various stages of the fatigue life of the specimen, the actual rate of crack growth could be determined. The crack was measured from the radiograph with an accuracy of approximately 0.01 inches. Due to the difficulty in accurately measuring the actual crack size, curves are drawn to approximately fit the crack propagation data in Figures 6.2 to 6.4 inclusive. Since it is difficult to measure small amounts of crack growth on the radiographs it is difficult also to pinpoint the time of crack initiation accurately.

6.4 Analysis of Crack Propagation Data

Using Eq. 1 with $n = 2.25$ and $C = 0.275 \times 10^{-8}$ or 0.66×10^{-8} to estimate the propagation lives for the specimens was not satisfactory. The computed values were not in very good agreement with the observed measurements of crack growth rate. The predicted growth rates from Eq. 1 were much shorter than the actual propagation rates. Therefore, it was necessary to determine a new set of constants for the material being used in the present study.

The values of C and n were determined from the plot of log (ΔK) vs. log (da/dN) for the various specimens. Values of ΔK at different crack dimensions and the corresponding slope of the a vs. N curves were determined for each of the three specimens so that a plot

of log (ΔK) vs. log (da/dN) could be obtained. The values of ΔK were computed using Eq. 3 and the corresponding slopes were computed as $\Delta a/\Delta N$ for small increments of a. The resulting log (ΔK) vs. log (da/dN) curve is presented in Figure 6.5. The value of n corresponds to the slope of the log (ΔK) vs. log (da/dN) curve, while C corresponds to the value of da/dN at $\Delta K = 1.0$. The best fit curve for the computed values of ΔK and da/dN was found using a least squares curve fitting procedure and is shown in Figure 6.5 with a two standard deviation band. The values of the constants C and n were then determined from the best fit curve and the two standard deviation bounds. The following expression for the rate of crack propagation resulted:

$$\frac{da}{dN} = C(\Delta K)^{5.8} \qquad (5)$$

where

$$0.134 \times 10^{-13} \leq C \leq 0.501 \times 10^{-13}$$

and ΔK is computed using Eq. 3.

The number of cycles of propagation to various crack sizes was computed by integrating Eq. 5 with $C = 0.134 \times 10^{-13}$ and $C = 0.501 \times 10^{-13}$, the bounds of two standard deviations, and $C = 0.269 \times 10^{-13}$ the best fit curve, using Simpson's rule for numerical integration. These three curves are drawn for each of the three specimens included in the crack propagation studies (Figures 6.6, 6.7, and 6.8). The measured data from these specimens (from the radiographs) are shown on the figures also. The data for specimen LP1-2-5 is best represented by the curves

with $C = 0.501 \times 10^{-13}$ and $C = 0.269 \times 10^{-13}$, while specimens LP1-2-1 and LP1-2-4 are best represented by the curves with $C = 0.269 \times 10^{-13}$ and $C = 0.134 \times 10^{-13}$.

Differences in the notch tip geometry or error in the crack measurement (an increase of 0.025 in. in original crack length would be sufficient) could easily account for the difference in crack propagation in specimen LP1-2-5 and the other specimens. If the initial range in stress intensity at the notch tip was greater for specimen LP1-2-5 than for the other specimens, the crack would initially propagate more quickly. Furthermore, since the initial size of the crack also affects the magnitude of the stress intensity, it too will affect the computed rate of crack propagation. Thus, both factors noted above could readily account for the lack of correlation in Figures 6.6 to 6.8.

If initiation of the fatigue cracks occurred as indicated in Figures 6.6, 6.7, and 6.8, a large portion of the specimen fatigue lives was spent in propagation of the cracks (see Table 6.5). More time was probably spent in propagation than was estimated from the measurements on the radiographs. However, this was not unexpected since, as explained earlier, the initiation point was difficult to determine.

A conservative estimate of the propagation life of the welded specimens (considered by some to be essentially the total fatigue life since such a large portion of the life is spent in propagation) can be obtained from the following equation.

$$\frac{da}{dN} = 0.501 \times 10^{-13} (\Delta K)^{5.8} \qquad (6)$$

where ΔK is given by Eq. 3. However there are a number of limitations on this expression so it should be used with caution. As pointed out previously, the values of n and C are sensitive to the environment so the expression is valid only for specimens tested in a room temperature air environment. The expression was developed for specimens loaded only from 0-to-tension and for a through crack in a finite plate. Various other formulas for computing ΔK are available in the literature[10,13] for other kinds of defects.

7. Summary and Conclusions

Much research has been conducted during the last 40 years or so on the fatigue behavior of welded connections, but only a small portion of the research has centered on the behavior of welds containing internal flaws. The purpose of this investigation was to conduct a study to gain a better understanding of the fatigue behavior of welds in mild steel containing defects. Since an important aspect of the fatigue behavior is the amount of time spent in initiation and in propagation of fatigue cracks starting from the defects, some of the fatigue test specimens were examined to determine a relationship to predict the crack propagation life of the specimens.

The types of defects that were investigated were two degrees of porosity and incomplete penetration. The degree of defect was related to the AWS Specifications[1] for bridge design. A more detailed description of these defects is given in section 3 and Figures 3.2 and 3.8. The S-N curves are presented (Figures 5.1 to 5.3) for the specimens with

defects and for a series of sound welded joints. Two of the four specimens tested with a small amount of porosity defect failed outside of the weld so the results of these two tests have been combined with the data for the sound welds. Thus, the data show that the presence of small amounts of porosity, approximately equivalent to the AWS Bridge Specification[1] limits, does not greatly reduce the fatigue strength of the weld from that of sound welded joints, while the large clusters of porosity and the lack of penetration do affect the fatigue strength significantly at the longer lives. However, the S-N curves for the joints with defects and the sound welds all tend to converge in the shorter life region. The results of the tests conducted in this program are compared in Figure 5.8 with the AASHO 1971 Specification[2] for bridge design.

Fatigue crack propagation rates have been studied extensively for high strength steels while for mild steel weld metal relatively little information is available. An attempt was made to use the existing relationships developed for high strength steels to predict the crack propagation rates for the specimens of this investigation with incomplete penetration. However, the predictions greatly underestimated the observed propagation life of the specimens. Using the observed data, an expression is provided to predict the propagation life of the specimens tested in this study. The critical factor in determining the rate of the crack growth is the range of stress intensity at the tip of the fatigue crack, a factor that is a function of the crack size and specimen geometry.

As a result of this investigation it may be concluded that:

1. Small defects or amounts of porosity did not greatly change the fatigue behavior of the

connection from that of a sound welded connection.

2. Large clusters of porosity or lack of penetration significantly reduced the fatigue strength of the connections at longer lives.
3. Connections designed in accordance with current specifications yielded a large factor of safety against failure, for sound welds and long lives. However, with severe defects the current specifications were generally unconservative at both short and long lives. The smallest factors of safety were found at the shorter lives.
4. The general expression:

$$\frac{da}{dN} = C\ (\Delta K)^n$$

is applicable for crack propagation in the tests of this investigation, with the values of C, n, and ΔK depending on the test conditions, and initial flaw.

5. The expression:

$$\frac{da}{dN} = 0.501 \times 10^{-13}\ (\Delta K)^{5.8}$$

gives a conservative estimate of the crack propagation in the connections cycled at high stresses and in a room temperature air environment.

6. The propagation life of the connections in mild steel welds could not be generalized to fit the relationships developed for high strength steels.

The amount of data obtained from this investigation was rather small and limited in its scope. However, it does provide information on the general pattern of behavior of defective welds cyclically loaded.

8. Acknowledgement

This report was prepared as a part of the Illinois Cooperative Highway Research Program, Project IHR-64, "Welded Highway Structures," by the Department of Civil Engineering, in the Engineering Experiment Station, University of Illinois at Urbana-Champaign, in cooperation with the Illinois Department of Transportation and the U.S. Department of Transportation, Federal Highway Administration.

Table 5.1

FATIGUE TESTING PROGRAM

Type of Defect	Number of Tests at Short Life	Long Life
Sound Weld	6	4
Porosity--AWS Allowable[1]	2	2
Porosity Severe	2	3
Lack of Penetration--3/16"	7	3
Totals	17	12

Table 5.2

SUMMARY OF FATIGUE TEST DATA

Specimen Number	Defect Type*	Gross Area Sq. In.	Gross Stress Range ksi	Net Area Sq. In.	Net Stress Range	Stress Ratio	Life in Thousands of Cycles	Location of Failure	Remarks
S1-1	S	0.996	33.0	--	--	+0.056	5,129.6+		No failure at initial stress cycle
S1-1A	S	0.996	38.0	--	--	+0.050	2,274.1+		No failure
S1-1B	S	0.996	43.7	--	--	+0.044	443.2	Weld metal	
S1-2	S	0.983	40.0	--	--	-0.111	630.8	Weld metal	
S1-3	S	1.007	40.0	--	--	-0.111	10,953.0+		No failure at initial stress cycle
S1-3A	S	1.007	46.0	--	--	-0.278	566.4	Base metal	
S1-4	S	0.974	46.0	--	--	-0.278	262.7	Weld metal	
S1-5	S	0.964	40.0	--	--	-0.111	2,691.8	Weld metal	
LP2-3-1	S	1.052	46.0	--	--	-0.278	75.1	Edge of weld metal	
LP2-3-2	S	1.048	46.0	--	--	-0.278	189.4	Edge of weld metal	
LP2-3-3	S	1.069	46.0	--	--	-0.278	289.0	Weld metal	
LP2-3-4	S	1.057	40.0	--	--	-0.111	275.7	Weld metal	
LP2-3-5	S	1.042	51.0	--	--	-0.417	51.4	Edge of weld metal	

Table 5.2 (Cont.)

Specimen Number	Defect Type*	Gross Area Sq. In.	Gross Stress Range ksi	Net Area Sq. In.	Net Stress Range	Stress Ratio	Life in Thousands of Cycles	Location of Failure	Remarks
PC4-1	PC	1.055	34.0	--	--	+0.056	1,485.5	Through defect	
PC4-2	PC	1.062	48.0	--	--	+0.056	5,353.8	Through defect	
PC4-3	PC	1.060	56.0	--	--	-0.333	392.9	In base metal	
PC4-4	PC	1.049	34.0	--	--	-0.556	107.1	In base metal	
PS5-1	PS	1.053	34.0	--	--	-0.056	713.3	Through defect	
PS5-2	PS	1.046	34.0	--	--	-0.056	325.5	Through defect	
PS5-3	PS	1.068	44.0	--	--	-0.222	80.3	Through defect	
PS5-4	PS	1.078	29.0	--	--	+0.195	633.0	Through defect	
PS5-5	PS	1.056	27.0	--	--	+0.250	1,024.9	Through defect	
LP1-2-1	LP	1.052	34.0	0.843	42.93	+0.056	133.1	Through defect	Used to study crack propagation
LP1-2-2	LP	1.038	20.0	0.783	26.54	+0.445	272.6	Through defect	
LP1-2-3	LP	1.032	16.9	0.792	22.0	+0.531	464.1	Through defect	
LP1-2-4	LP	1.038	34.0	0.752	46.8	+0.056	157.0	Through defect	Used to study crack propagation

Table 5.2 (Cont.)

Specimen Number	Defect Type*	Gross Area Sq. In.	Gross Stress Range ksi	Net Area Sq. In.	Net Stress Range	Stress Ratio	Life in Thousands of Cycles	Location of Failure	Remarks
LP1-2-5	LP	1.058	34.0	0.815	44.0	+0.056	90.8	Through defect	Used to study crack propagation
LP2-6-6	LP	1.056	34.0	0.818	43.8	+0.056	50.2	Through defect	
LP2-6-7	LP	1.072	16.0	0.833	20.6	+0.111	4,500.0+		No failures, broken statically
LP2-6-8	LP	1.044	22.0	0.716	32.1	+0.389	167.0	Through defect	
LP2-6-9	LP	1.033	14.0	0.719	31.7	+0.613	5,700.7+		No failure at initial stress cycle
LP2-6-9A	LP	1.033	34.0	0.719	48.8	+0.056	469.9	Through defect	
LP2-6-10	LP	1.036	15.0	0.706	22.0	+0.584	216.8	Through defect	

* S Denotes sound weld

PC Denotes porosity at AWS Specification[1] allowable

PS Denotes severe porosity (see photos of fracture surfaces--Appendix B)

LP Denotes lack of penetration (see photos of fracture surfaces--Appendix B)

Table 5.3

SUMMARY OF FATIGUE STRENGTHS OF CONNECTIONS
(Stress Range)

Weld Type	$F_{100,000}$ ksi	$2\sigma^*$ ksi	$F_{500,000}$ ksi	$2\sigma^*$ ksi	$F_{2,000,000}$ ksi	$2\sigma^*$ ksi
Sound	47.5	+3.4 -3.2	43.2	+3.1 -2.9	39.9	+2.8 -2.7
Severe Porosity	42.3	+5.8 -5.1	32.0	+4.4 -3.8	25.2	+3.4 -3.0
Lack of Penetration	30.4	+11.0 -8.1	20.1	+7.3 -5.3	14.1	+5.1 -3.7

* Two standard deviation

Table 6.1

SPECIMEN DETAILS

Specimen Number	Thickness	Defect Size	Gross Stress Range
LP1-2-1	0.704 in.	0.140 in.	2.0 - 36.0 ksi
LP1-2-4	0.694 in.	0.170 in.	2.0 - 36.0 ksi
LP1-2-5	0.704 in.	0.160 in.	2.0 - 36.0 ksi

Table 6.2

CRACK PROPAGATION DATA SPECIMEN LP1-2-1

X-ray Number	a	$N_{,Total}$	$N_{,Propagation}$
LP1-2-1S	0.07	56,000	0
LP1-2-1T	0.075	58,000	2,000
LP1-2-1U	0.075	60,000	4,000
LP1-2-1V	0.085	62,000	6,000
LP1-2-1W	0.085	64,000	8,000
LP1-2-1X	0.085	66,000	10,000
LP1-2-1Y	0.090	68,000	12,000
LP1-2-1Z	0.090	70,000	14,000
LP1-2-1A	0.090	75,000	19,000
LP1-2-1B	0.090	80,000	24,000
LP1-2-1C	0.095	85,000	29,000
LP1-2-1D	0.105	90,000	34,000
LP1-2-1F	0.105	101,500	45,500
LP1-2-1G	0.115	110,000	54,000
LP1-2-1H	0.115	115,000	59,000
LP1-2-1J	0.125	120,000	64,000
LP1-2-1K	0.160	130,000	74,000
LP1-2-1L	0.185	131,000	75,000
LP1-2-1M	0.20	132,100	76,100
LP1-2-1N	0.23	132,700	76,700
LP1-2-1P	0.25	133,100	77,100

Initial a = 0.07 inches (1/2 crack depth)
N = number of cycles
No crack growth measured to N = 56,000

Table 6.3

CRACK PROPAGATION DATA SPECIMEN LP1-2-4

X-ray Number	a	$N_{,Total}$	$N_{,Propagation}$
LP1-2-4F	0.085	95,200	0
LP1-2-4G	0.090	100,100	4,900
LP1-2-4H	0.090	105,000	9,800
LP1-2-4J	0.095	110,000	14,800
LP1-2-4K	0.115	115,000	19,800
LP1-2-4L	0.12	120,000	24,800
LP1-2-4M	0.12	125,200	30,000
LP1-2-4N	0.13	130,000	34,800
LP1-2-4O	0.13	135,000	39,800
LP1-2-4P	0.14	140,000	44,800
LP1-2-4Q	0.17	150,000	54,800
LP1-2-4R	0.18	152,000	56,800
LP1-2-4S	0.19	154,000	58,800
LP1-2-4T	0.205	155,500	60,300
LP1-2-4U	0.25	157,000	61,800

Initial a = 0.085 inches
N = number of cycles
No crack growth measured to N = 95,200 cycles

Table 6.4

CRACK PROPAGATION DATA SPECIMEN LP1-2-5

X-ray Number	a	$N_{,Total}$	$N_{,Propagation}$
LP1-2-5A	0.08	50,500	0
LP1-2-5B	0.095	70,100	19,600
LP1-2-5C	0.160	85,300	34,800
LP1-2-5D	0.260	90,800	40,300

Initial a = 0.08 inches
N = number of cycles

Table 6.5

COMPARISON OF MEASURED AND CALCULATED
CRACK PROPAGATION LIVES

Specimen Number	Initiation Period, Measured, Cycles	Crack Propagation Life, Measured Cycles	Crack Propagation, Life, Calculated, Cycles
LP1-2-1	56,000	77,100	94,400
LP1-2-4	95,200	61,800	54,100
LP1-2-5	50,500	40,300	65,400

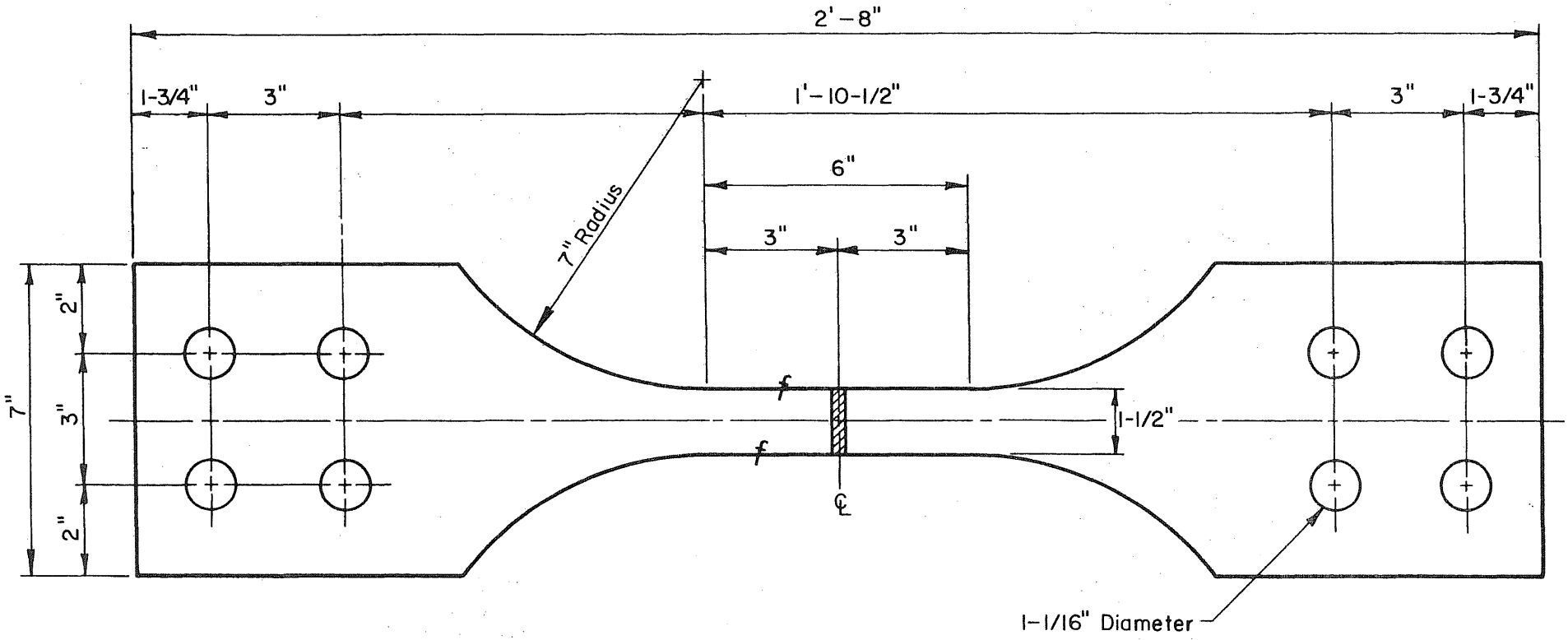

Note : Weld Reinforcement Machined Off and the Surfaces Polished In A Direction Perpendicular to the Axis of the Weld

FIG. 3.1 SPECIMEN FOR FATIGUE TEST

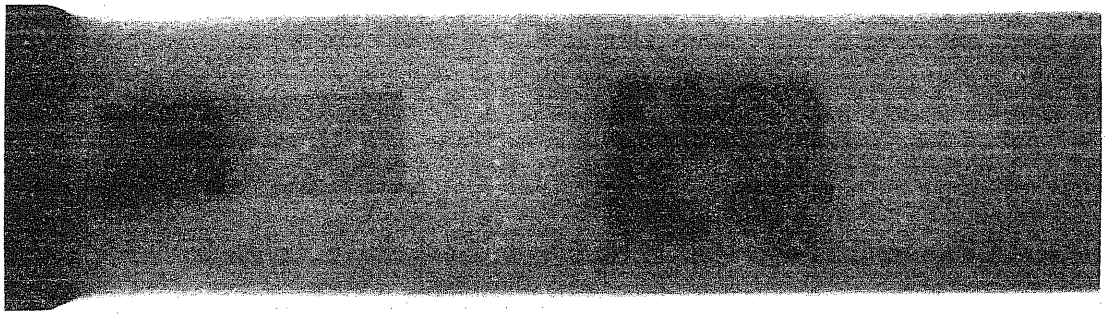

(a) Porosity Approximately At AWS Specification Allowable

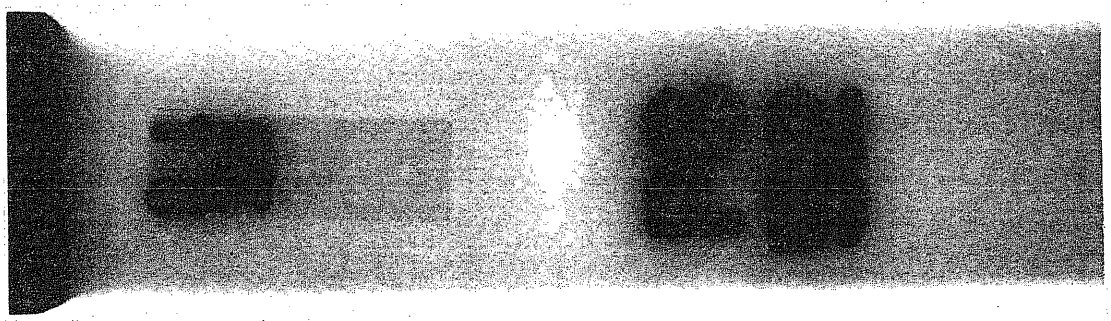

(b) Severe Cluster Of Porosity

FIG. 3.2 RADIOGRAPHIC EXAMPLES OF POROSITY DEFECTS

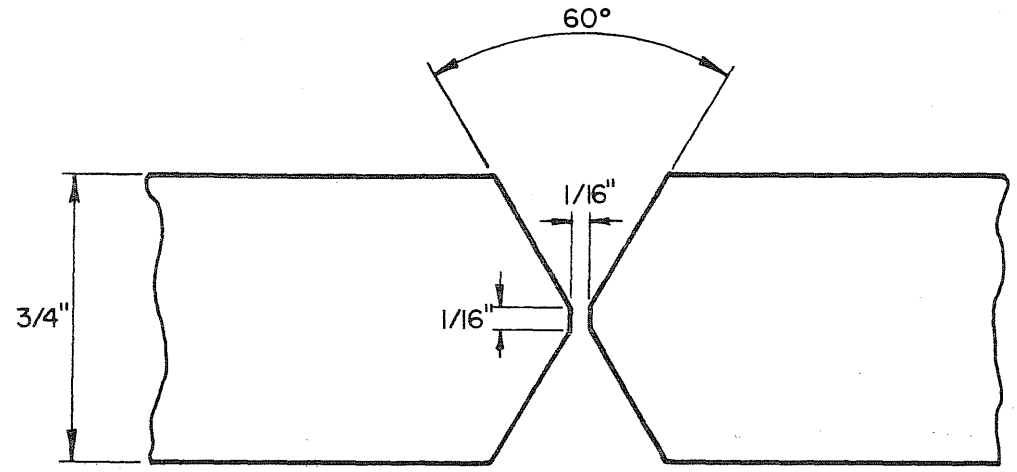

(a) V – Groove

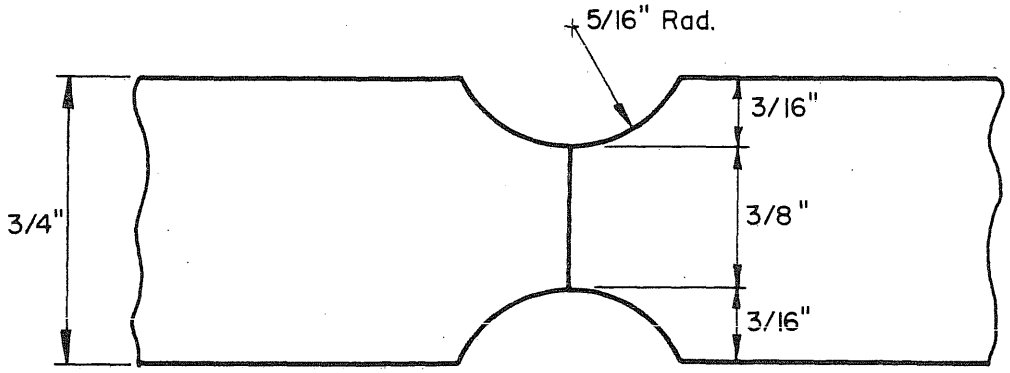

(b) U – Groove Type I

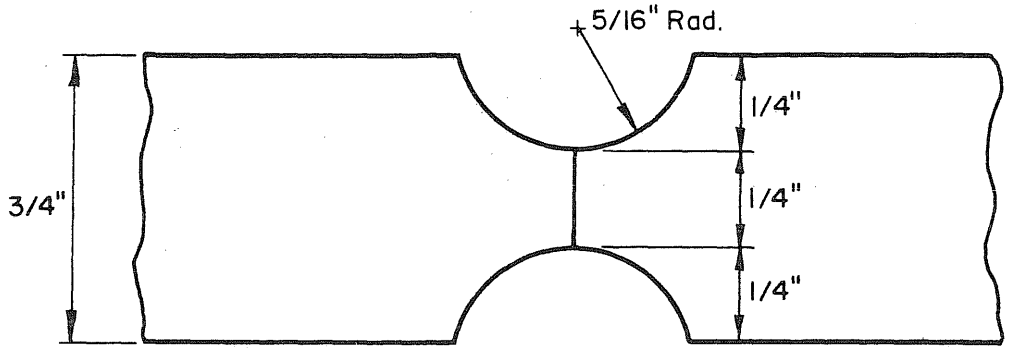

(c) U – Groove Type II

FIG. 3.3 DETAILS OF WELD GROOVES

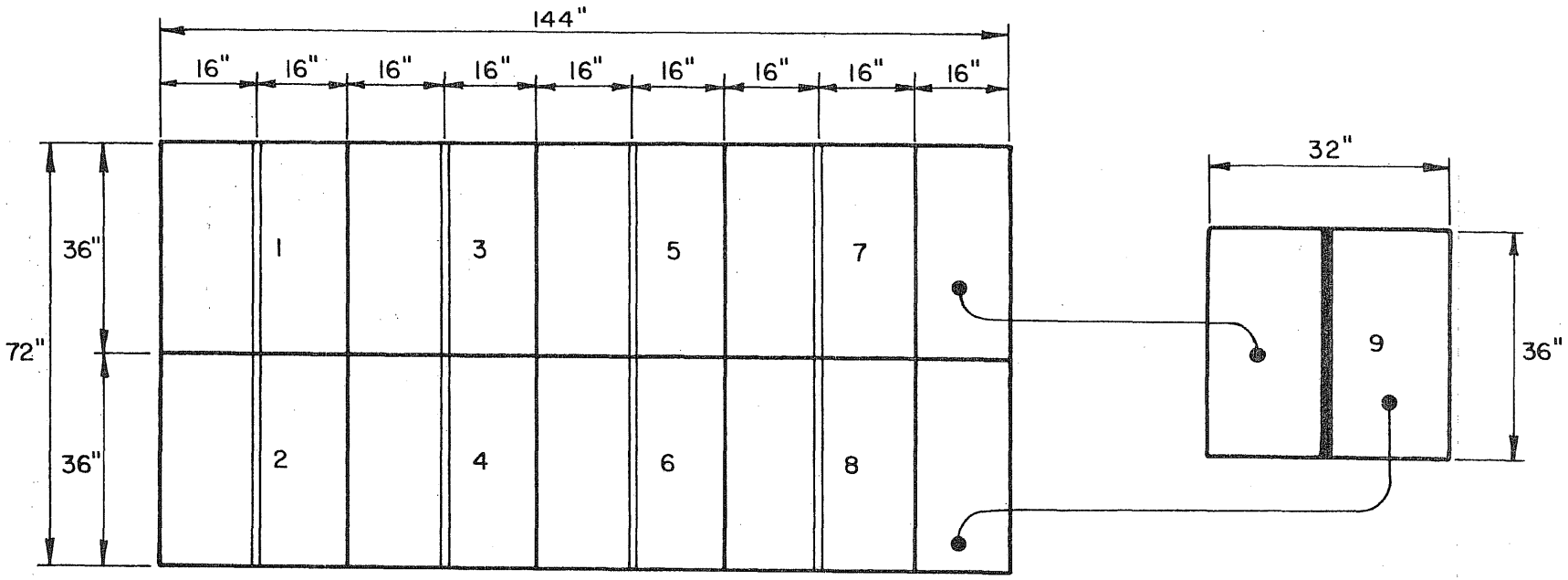

Plate Number A77
3/4" PL A36 Steel

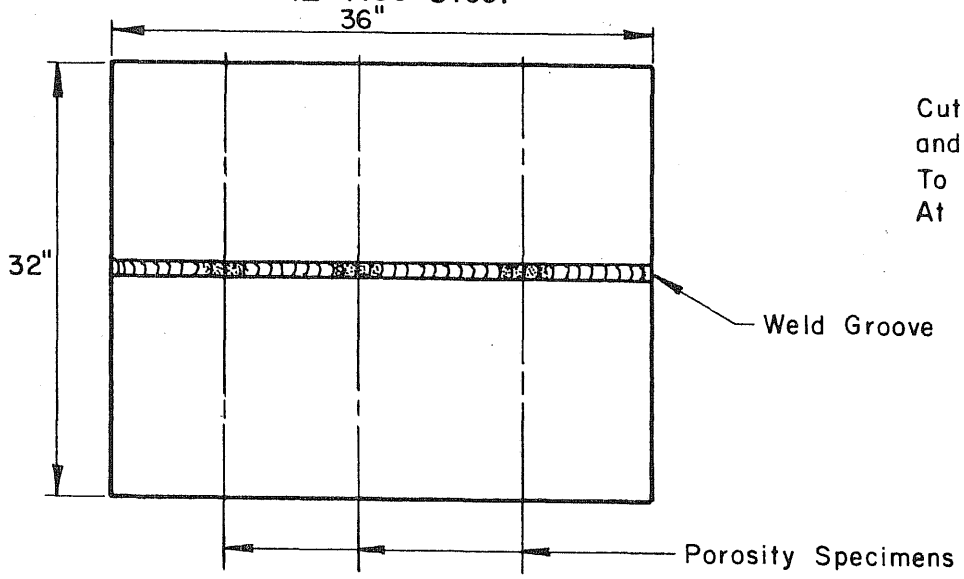

Cut Plate Into 36" x 16" Blocks. Bevel Edges and Weld Full 36" Length. Radiograph Weld To Locate Defects and Then Center Specimens At Severity of Defect Desired.

FIG. 3.4 CUTTING OF STEEL PLATE FOR WELDING

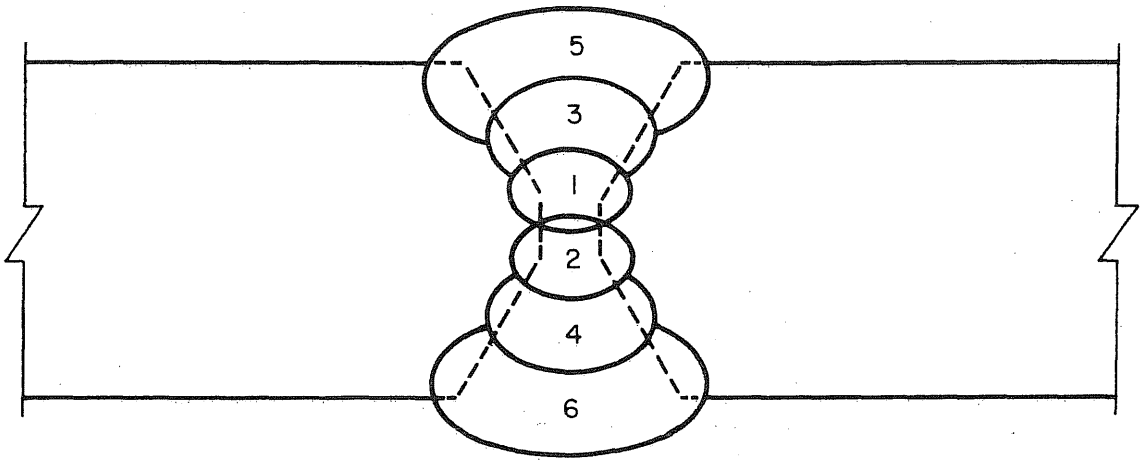

FIG. 3.5 SEQUENCE OF WELD PASSES

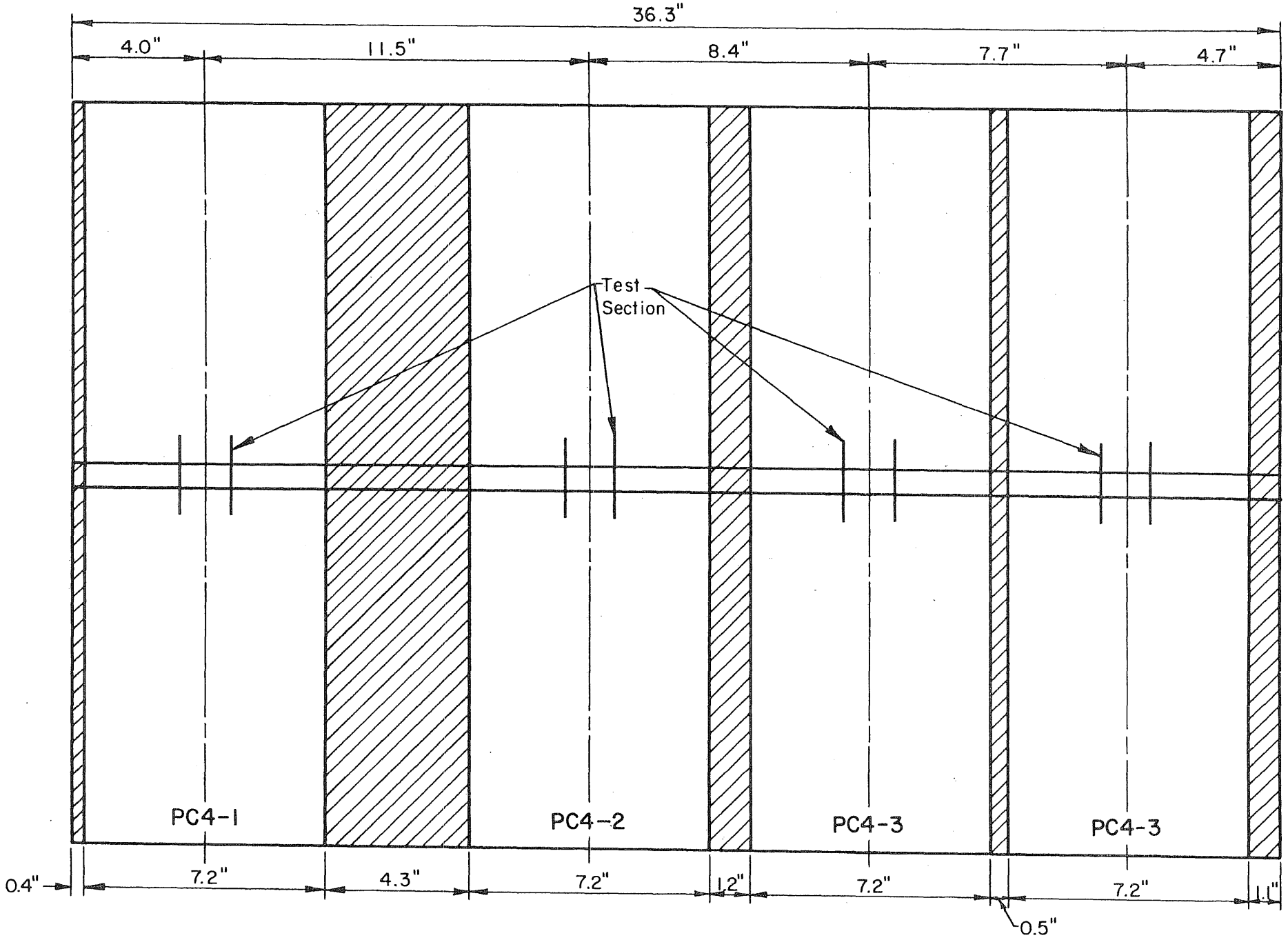

FIG. 3.6 LOCATIONS FOR CUTTING OF TEST SPECIMENS FROM WELDED PLATE NO. 4

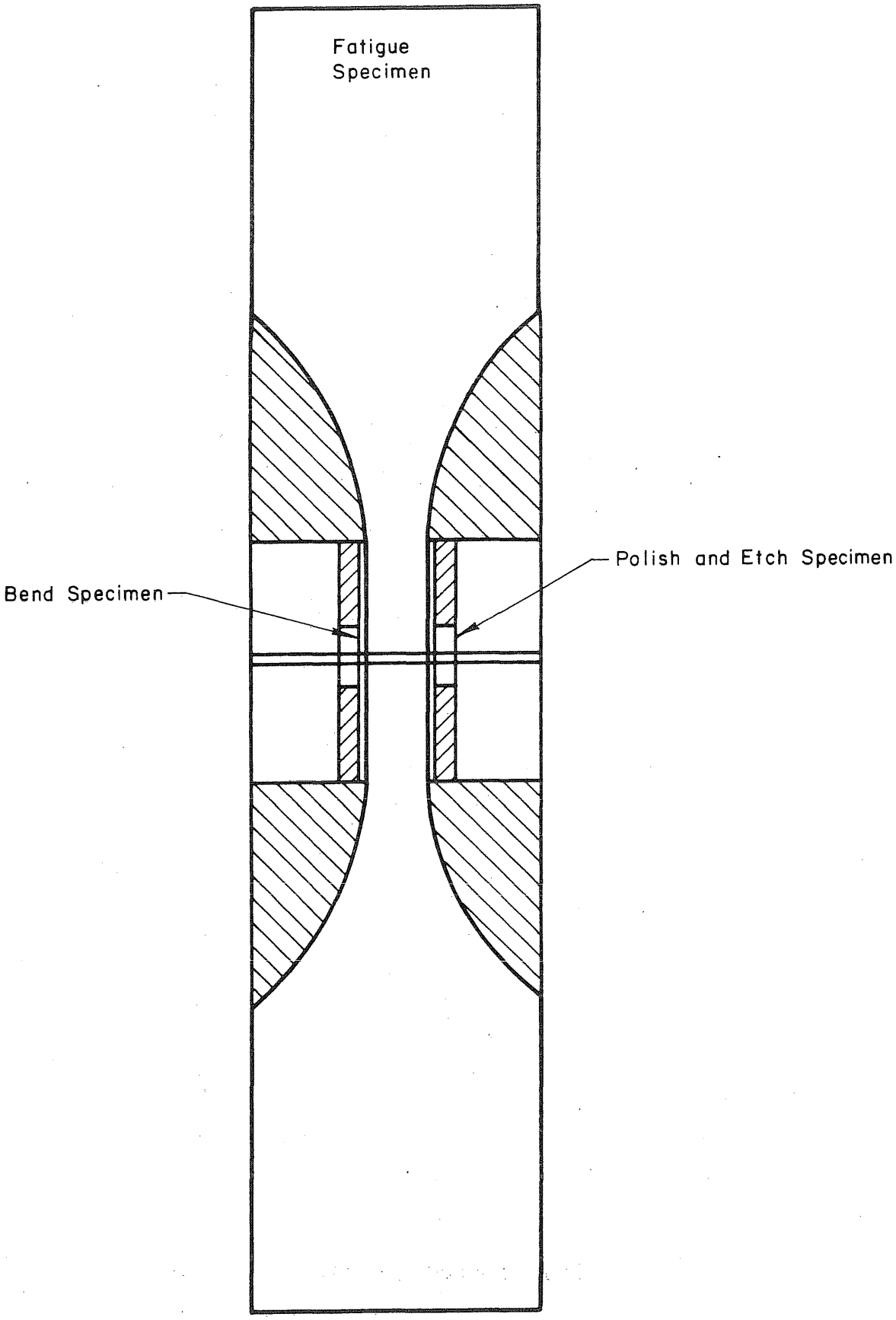

FIG. 3.7 LOCATION OF SPECIMENS FOR PARTIAL PENETRATION WELDS

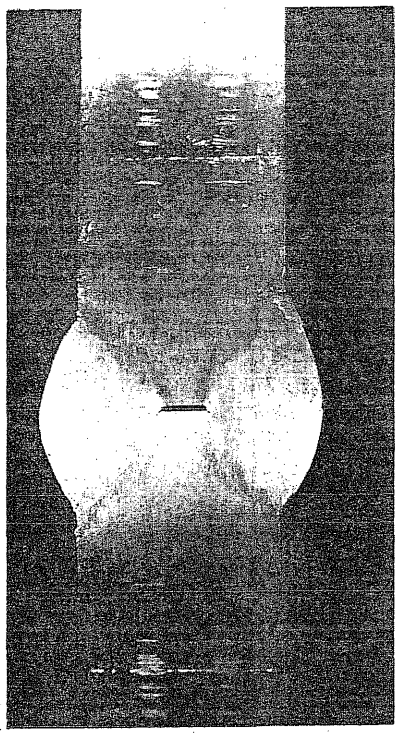

(a) Bend Specimen
(After Bending)

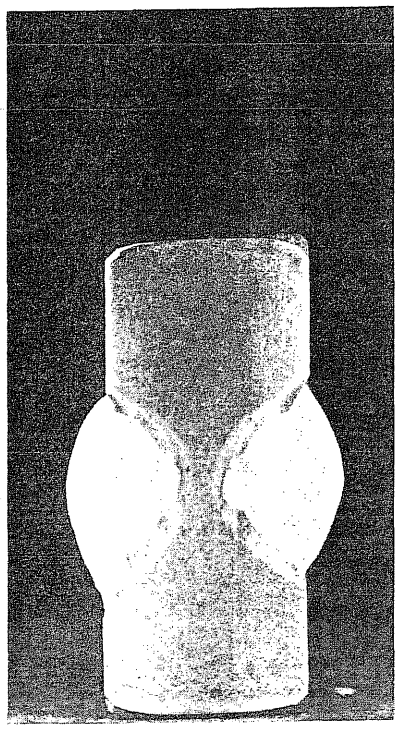

(b) Polished and Etched Specimen

FIG. 3.8 SPECIMENS SHOWING THE DEGREE OF LACK OF PENETRATION IN FATIGUE TEST SPECIMENS

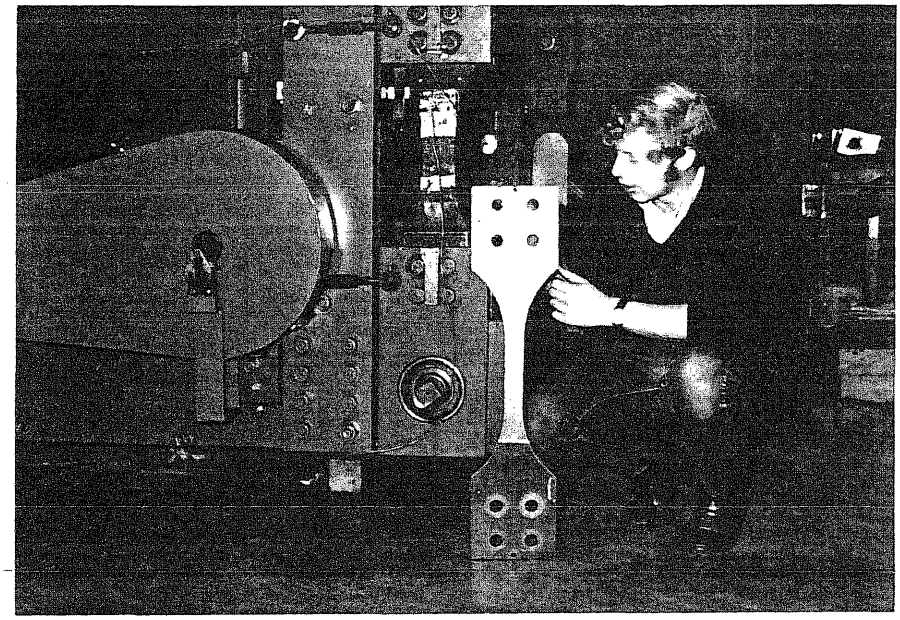

FIG. 3.9 PHOTOGRAPH OF SPECIMEN AS MACHINED AND TESTED

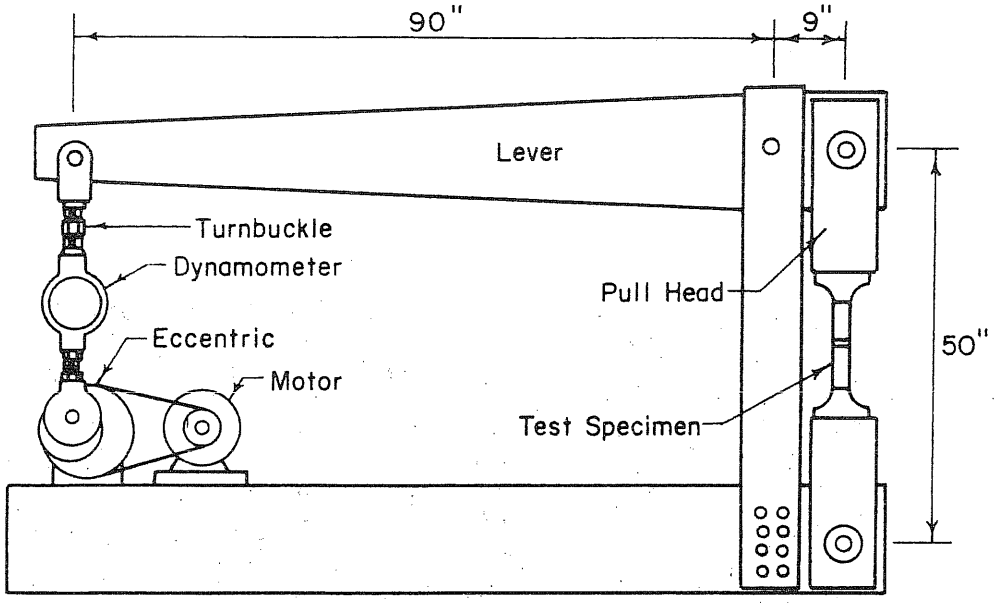

(a) Schematic Drawing

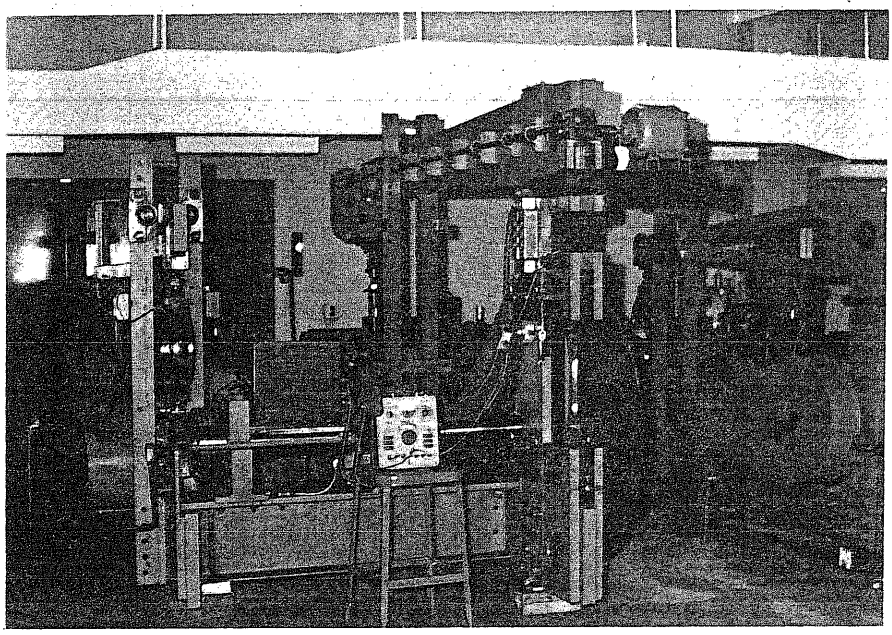

(b) Photograph

FIG. 4.1 FATIGUE MACHINES

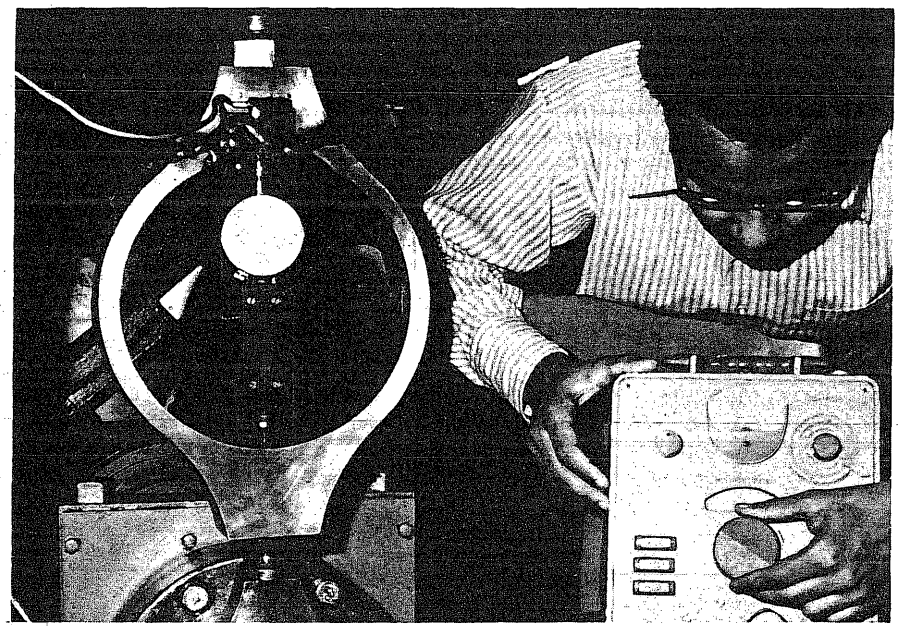

FIG. 4.2 PHOTOGRAPH OF DYNAMOMETER AND LOAD INDICATION INSTRUMENTS

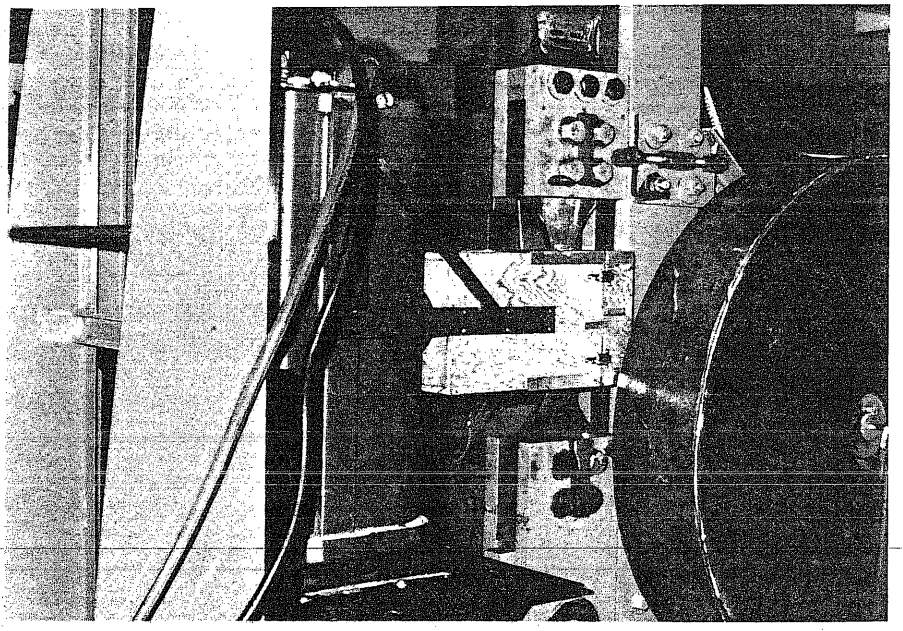

FIG. 4.3 X-RAY EQUIPMENT FOR CRACK PROPAGATION STUDIES

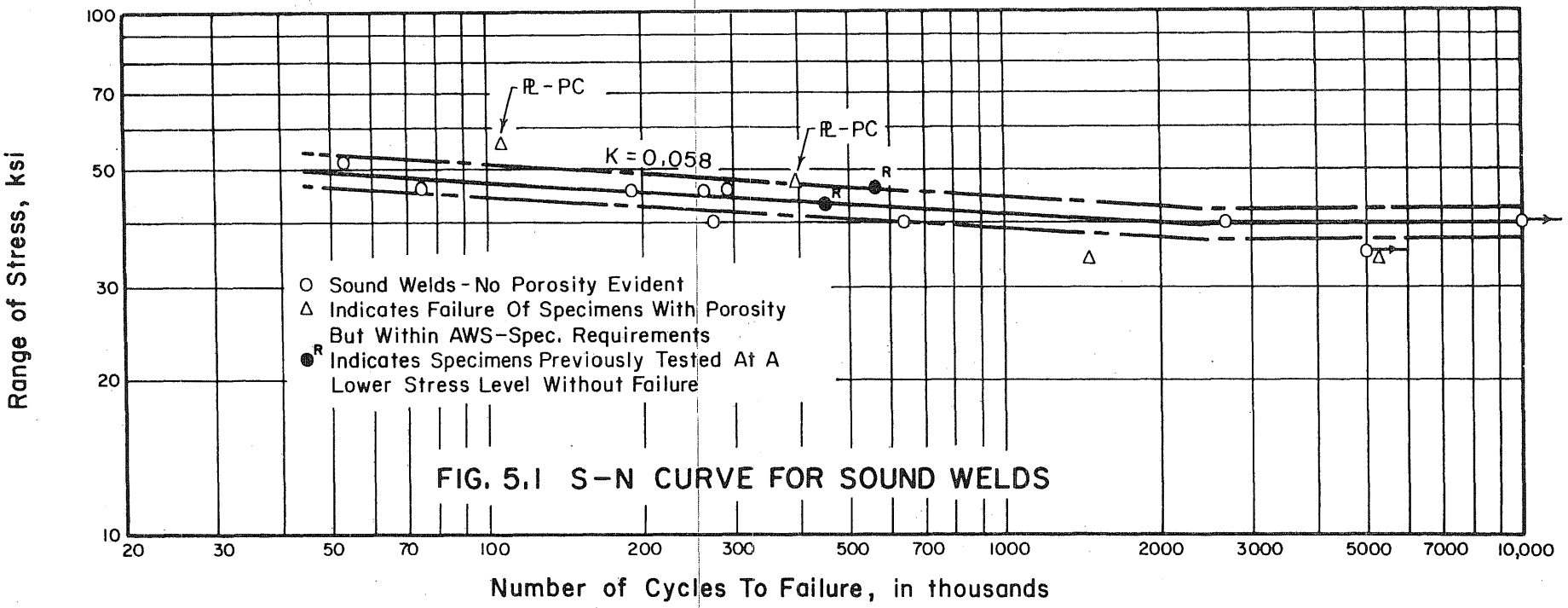

FIG. 5.1 S-N CURVE FOR SOUND WELDS

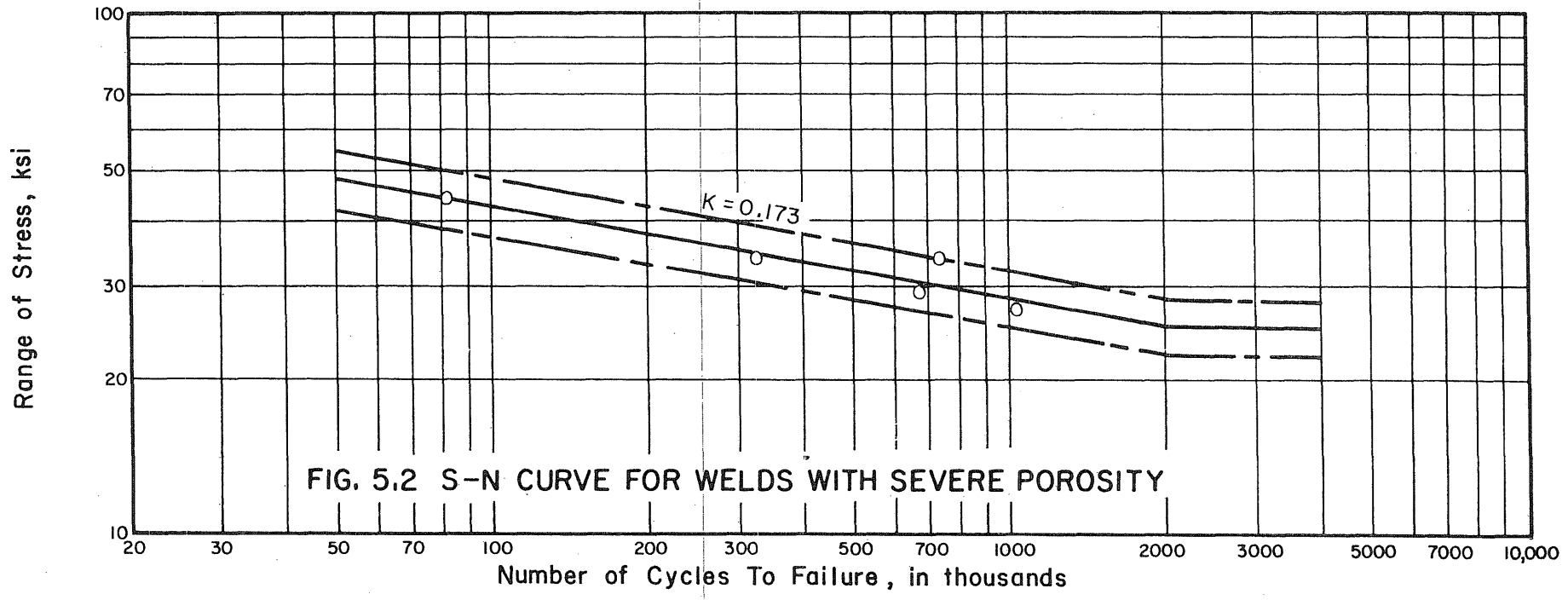

FIG. 5.2 S-N CURVE FOR WELDS WITH SEVERE POROSITY

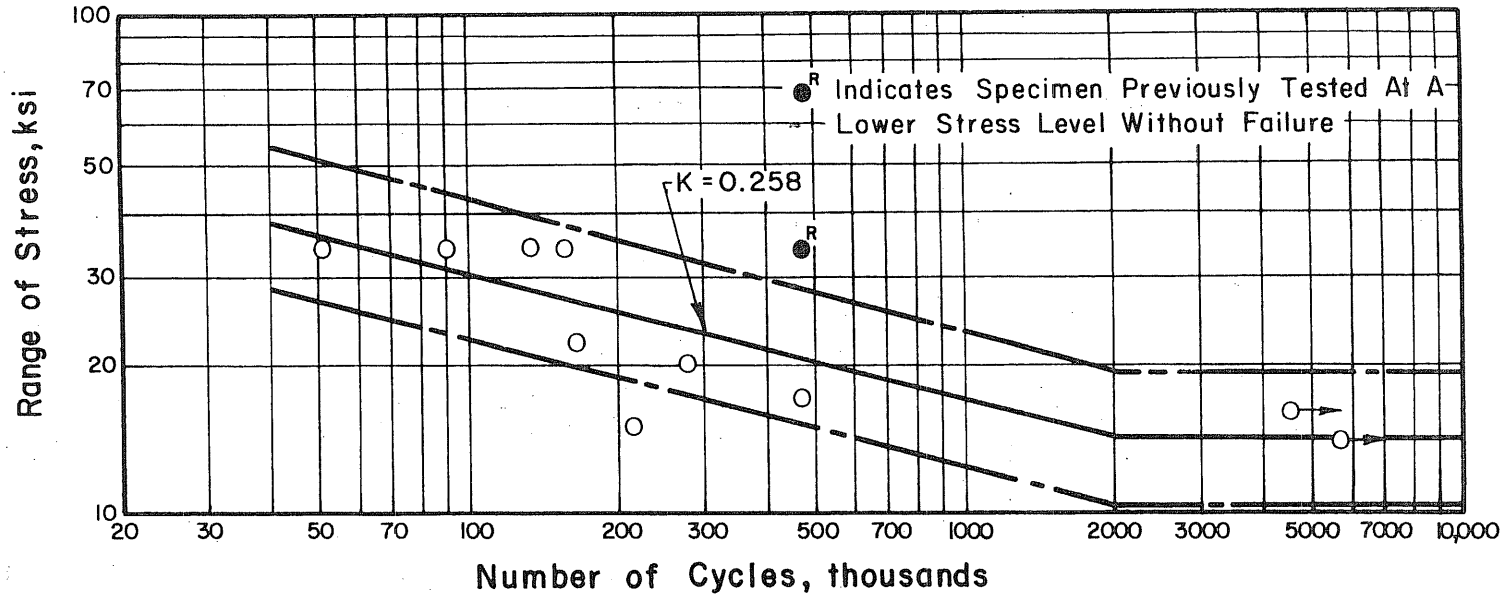

FIG. 5.3 S-N CURVE FOR WELDS WITH 3/16" LACK OF PENETRATION-GROSS STRESS RANGE

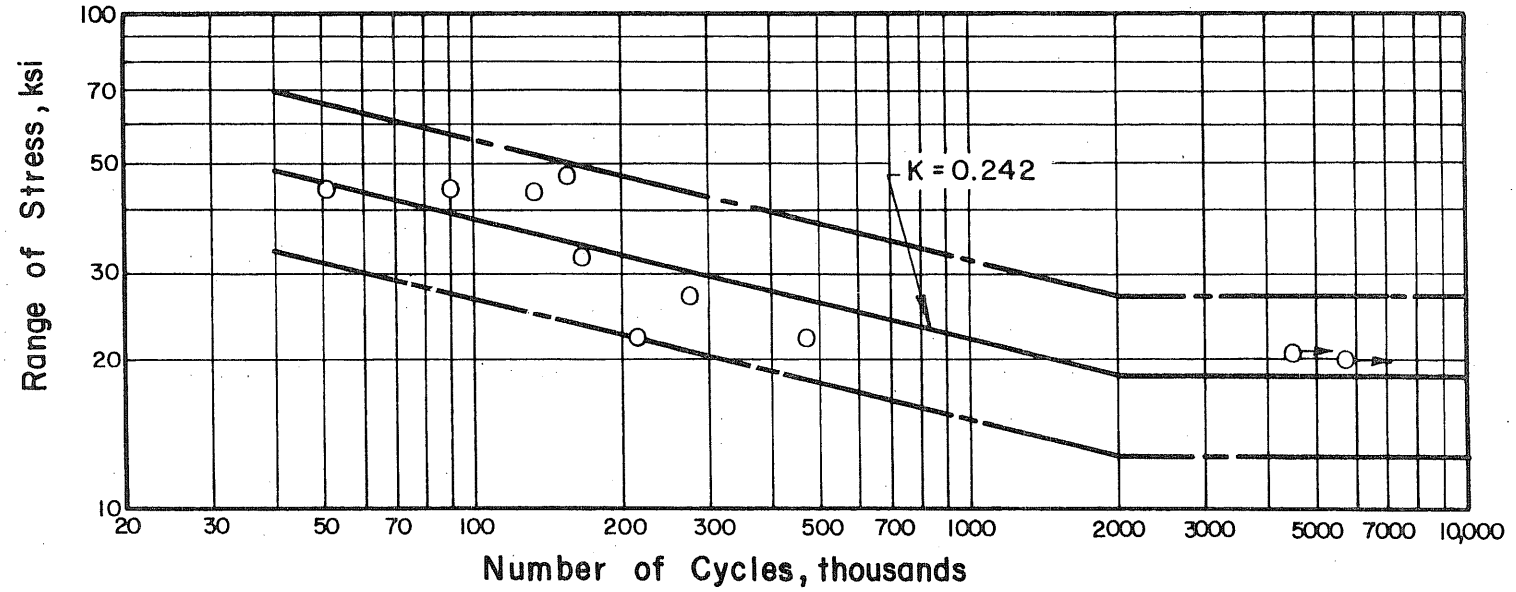

FIG. 5.4 S-N CURVE FOR WELDS WITH 3/16" LACK OF PENETRATION-NET STRESS RANGE

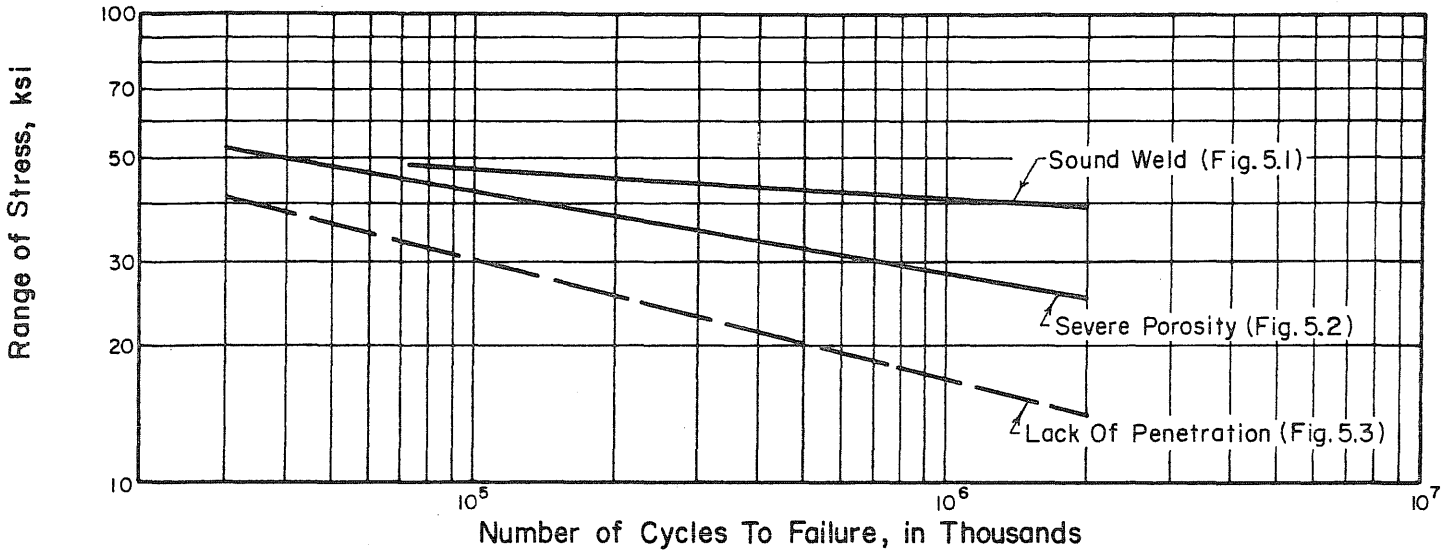

FIG. 5.5 COMBINED S-N CURVE FOR TEST DATA

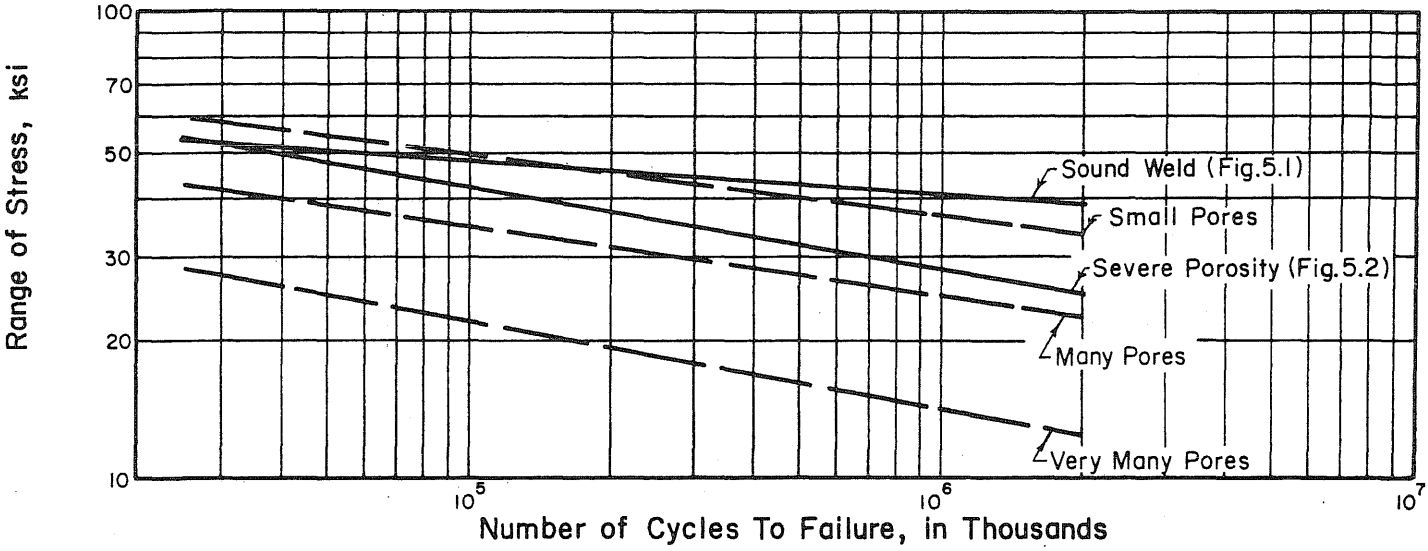

FIG. 5.6 COMPARISON OF TEST RESULTS FROM PRESENT STUDY WITH THOSE FOUND IN THE LITERATURE. POROSITY DEFECTS

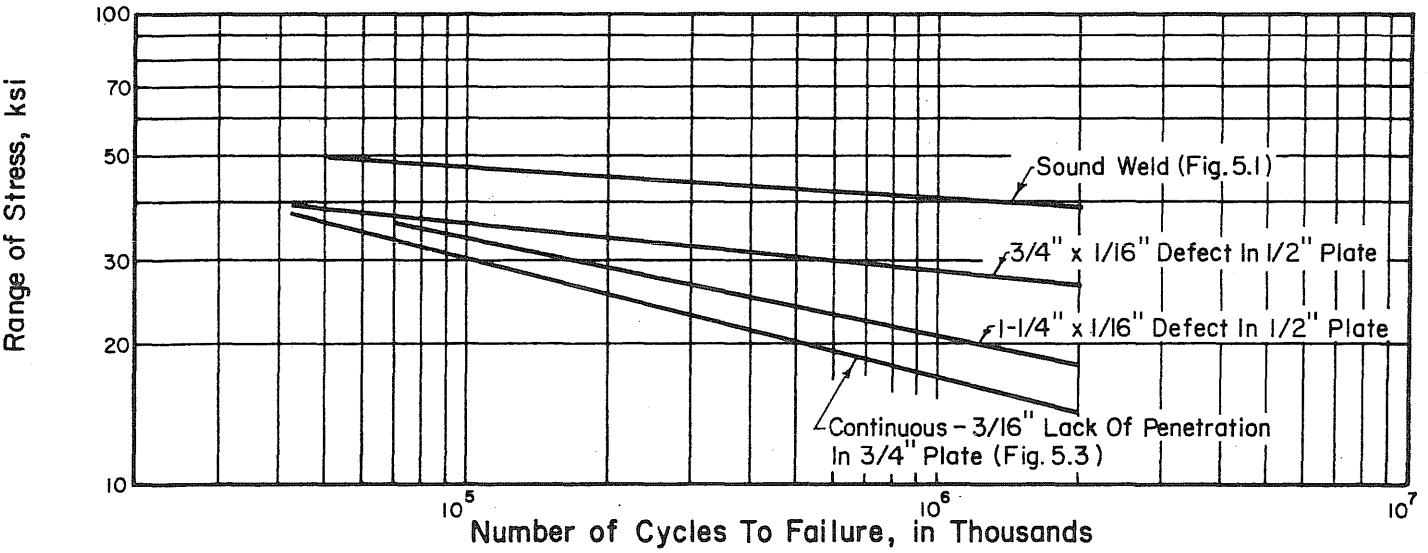

FIG. 5.7 COMPARISON OF TEST RESULTS FROM PRESENT STUDY WITH THOSE FOUND IN THE LITERATURE. LACK OF PENE. DEFECT

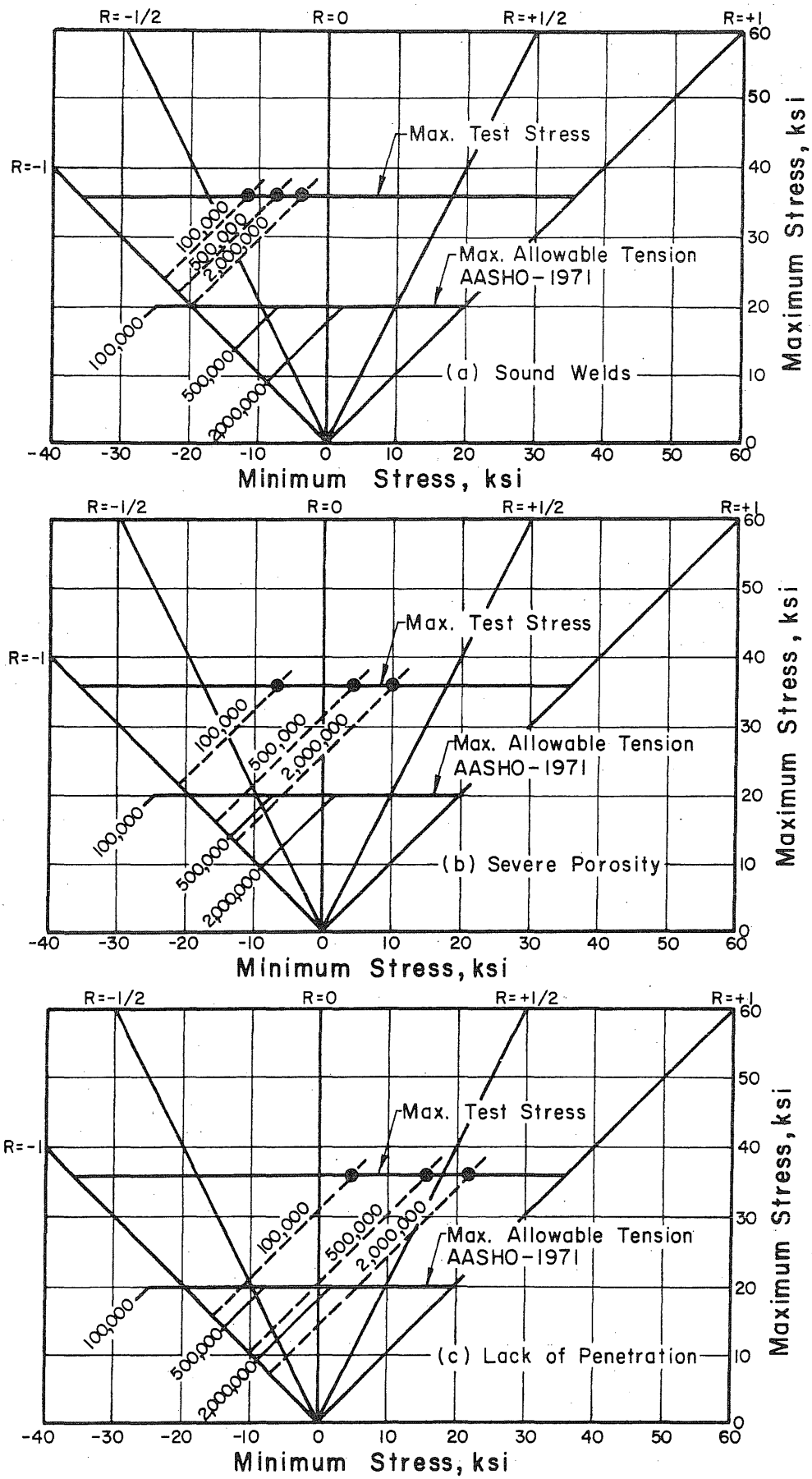

FIG. 5.8 MODIFIED GOODMAN FATIGUE DIAGRAM. COMPARISON OF TEST RESULTS WITH AASHO-1971 DESIGN REQUIREMENTS

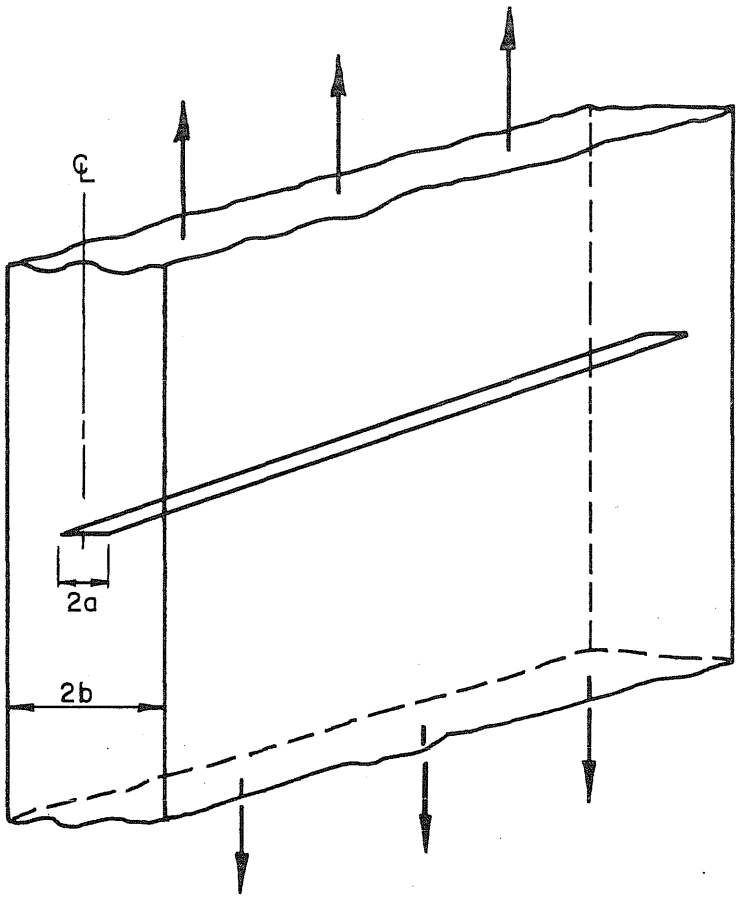

FIG. 6.1 MODEL FOR TEST SPECIMENS IN CRACK PROPAGATION STUDY

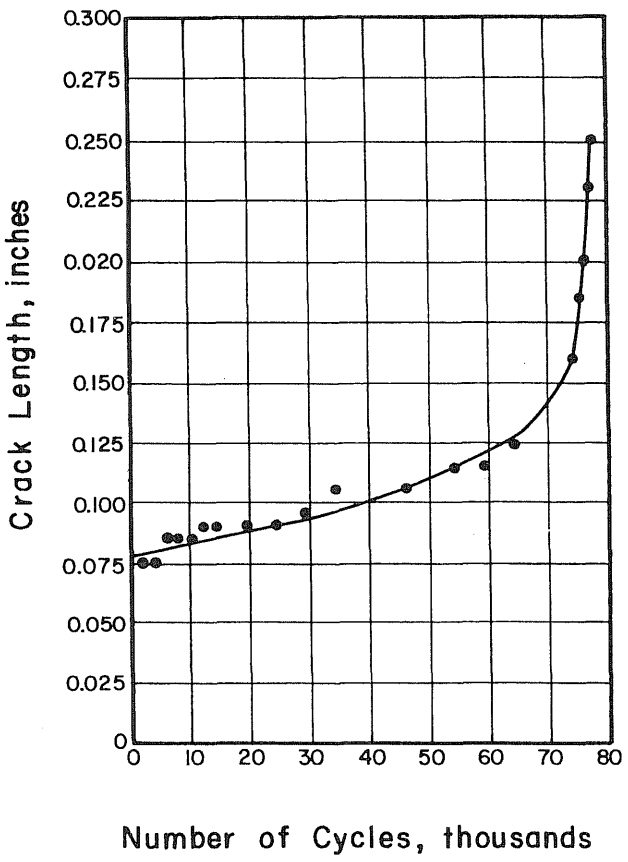

FIG. 6.2 SPECIMEN LPI-2-1. PROPAGATION MEASUREMENTS TAKEN FROM RADIOGRAPHS

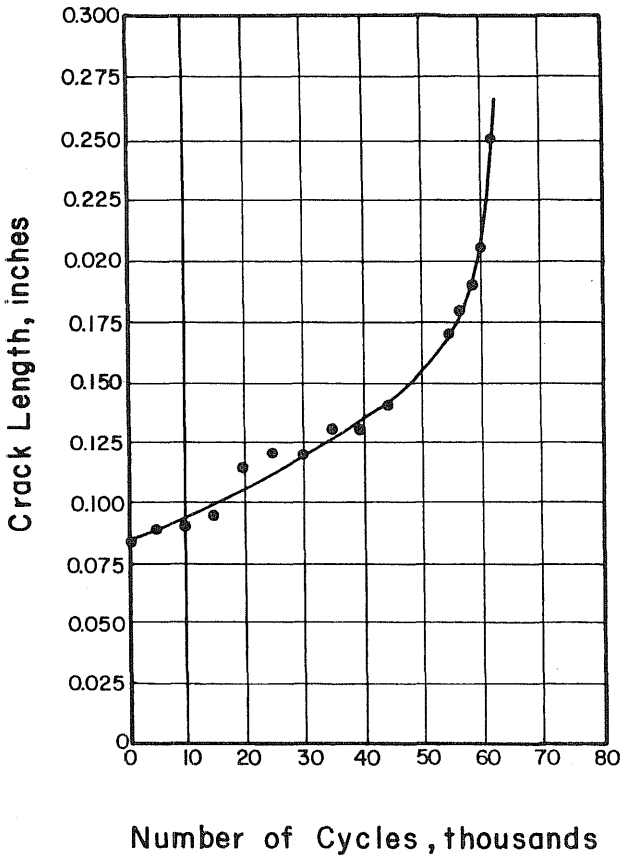

FIG. 6.3 SPECIMEN LPI-2-4. PROPAGATION MEASUREMENTS TAKEN FROM RADIOGRAPHS

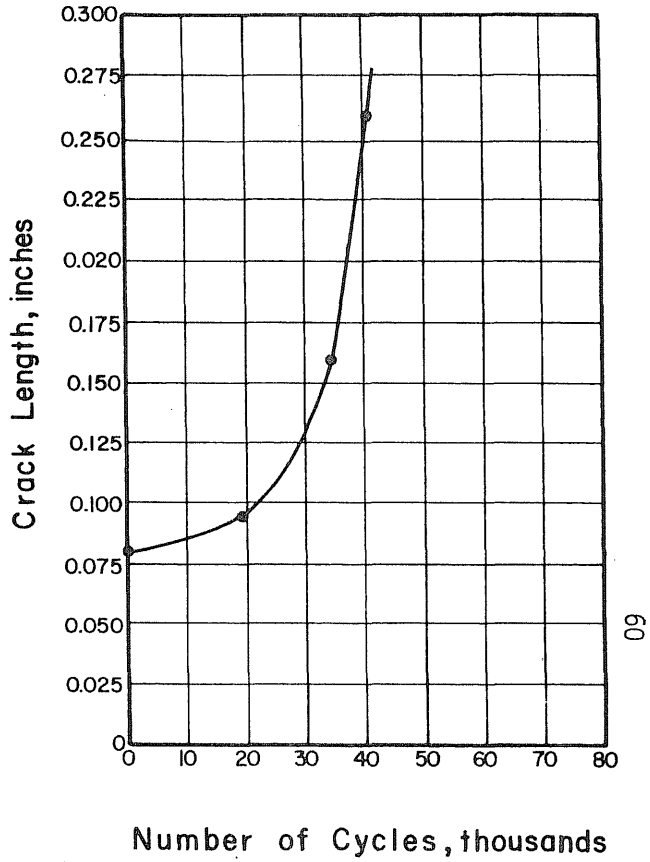

FIG. 6.4 SPECIMEN LPI-2-5. PROPAGATION MEASUREMENTS TAKEN FROM RADIOGRAPHS

PROPAGATION MEASUREMENTS TAKEN FROM RADIOGRAPHS

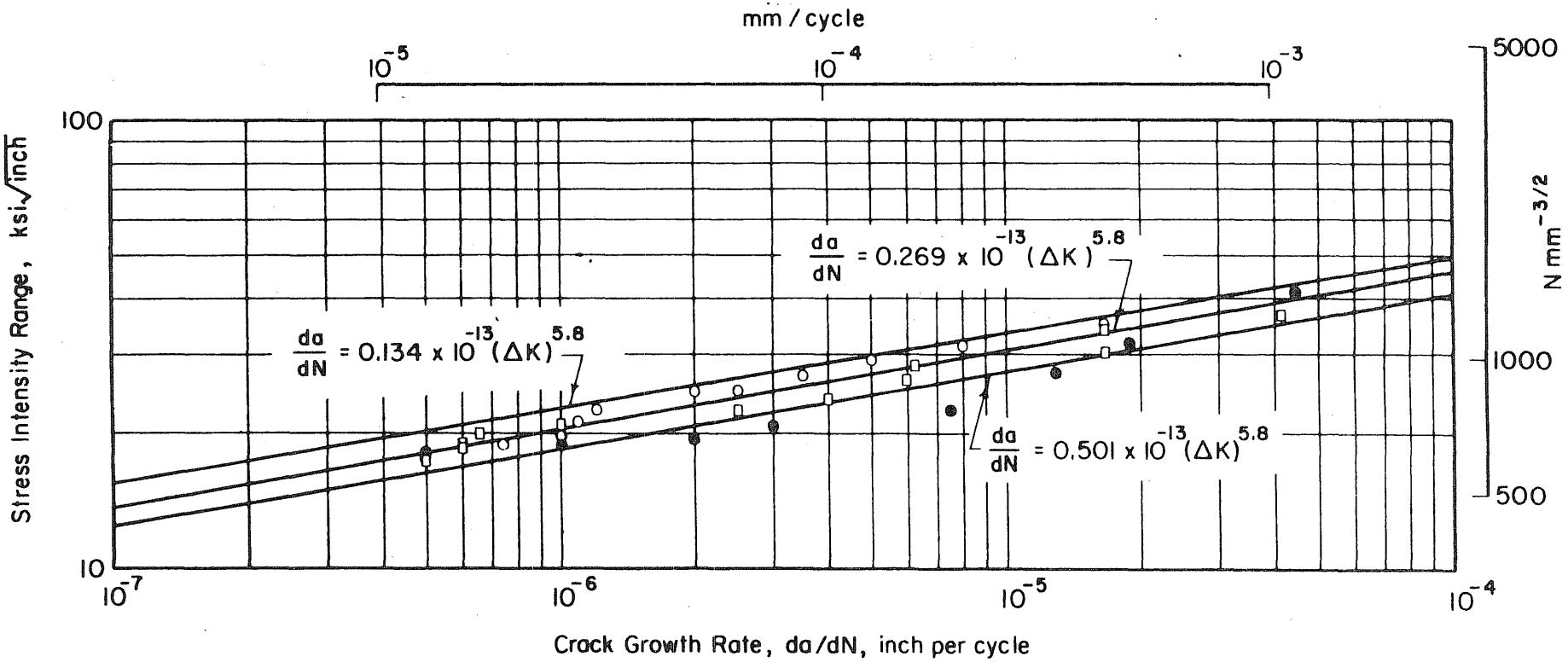

FIG. 6.5 PLOT OF LOG (ΔK) VS. LOG (da/dN)

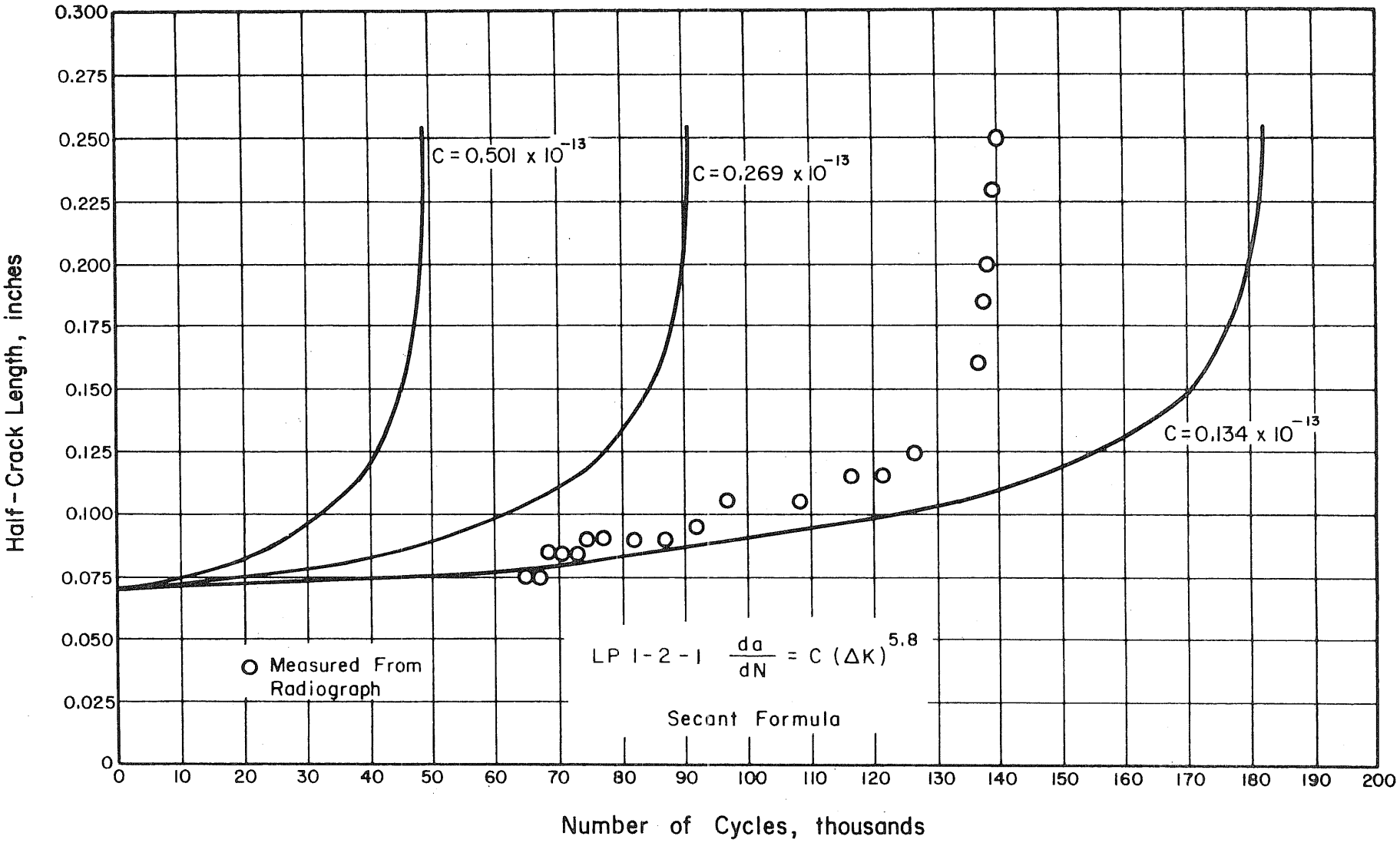

FIG. 6.6 COMPUTED CRACK PROPAGATION CURVES FOR SPECIMEN LP 1-2-1

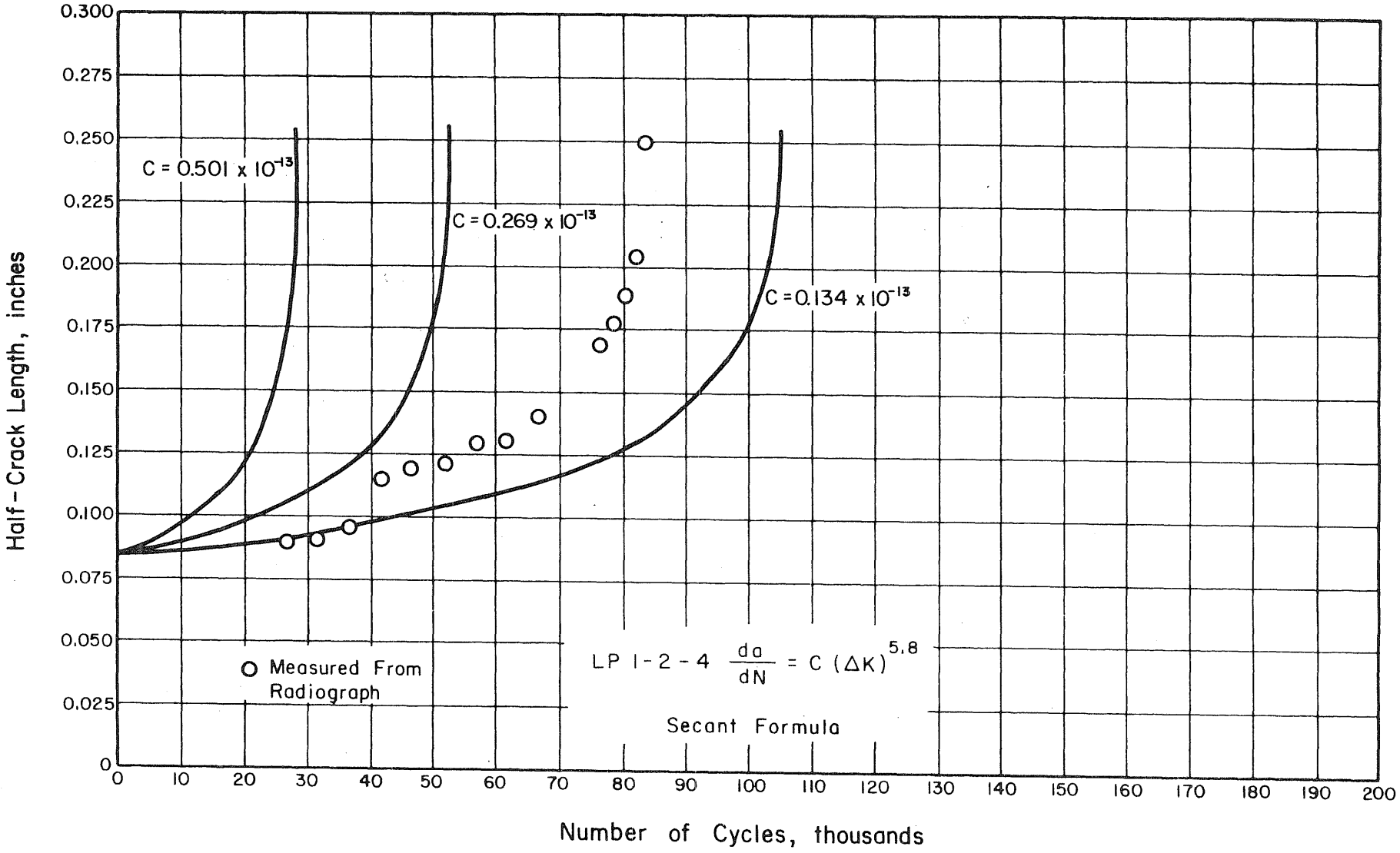

FIG. 6.7 COMPUTED CRACK PROPAGATION CURVES FOR SPECIMEN LP 1-2-4

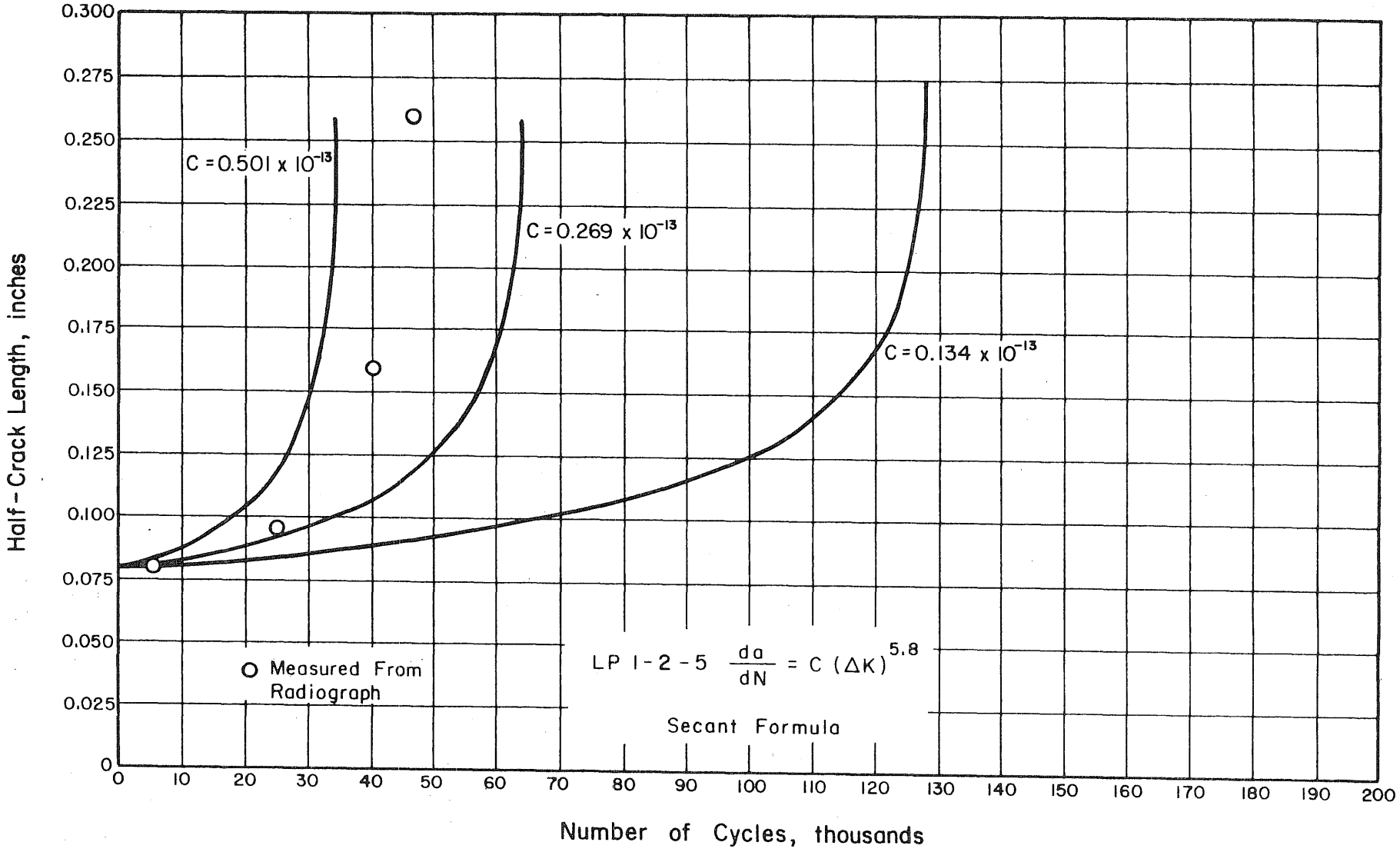

FIG. 6.8 COMPUTED CRACK PROPAGATION CURVES FOR SPECIMEN LP 1-2-5

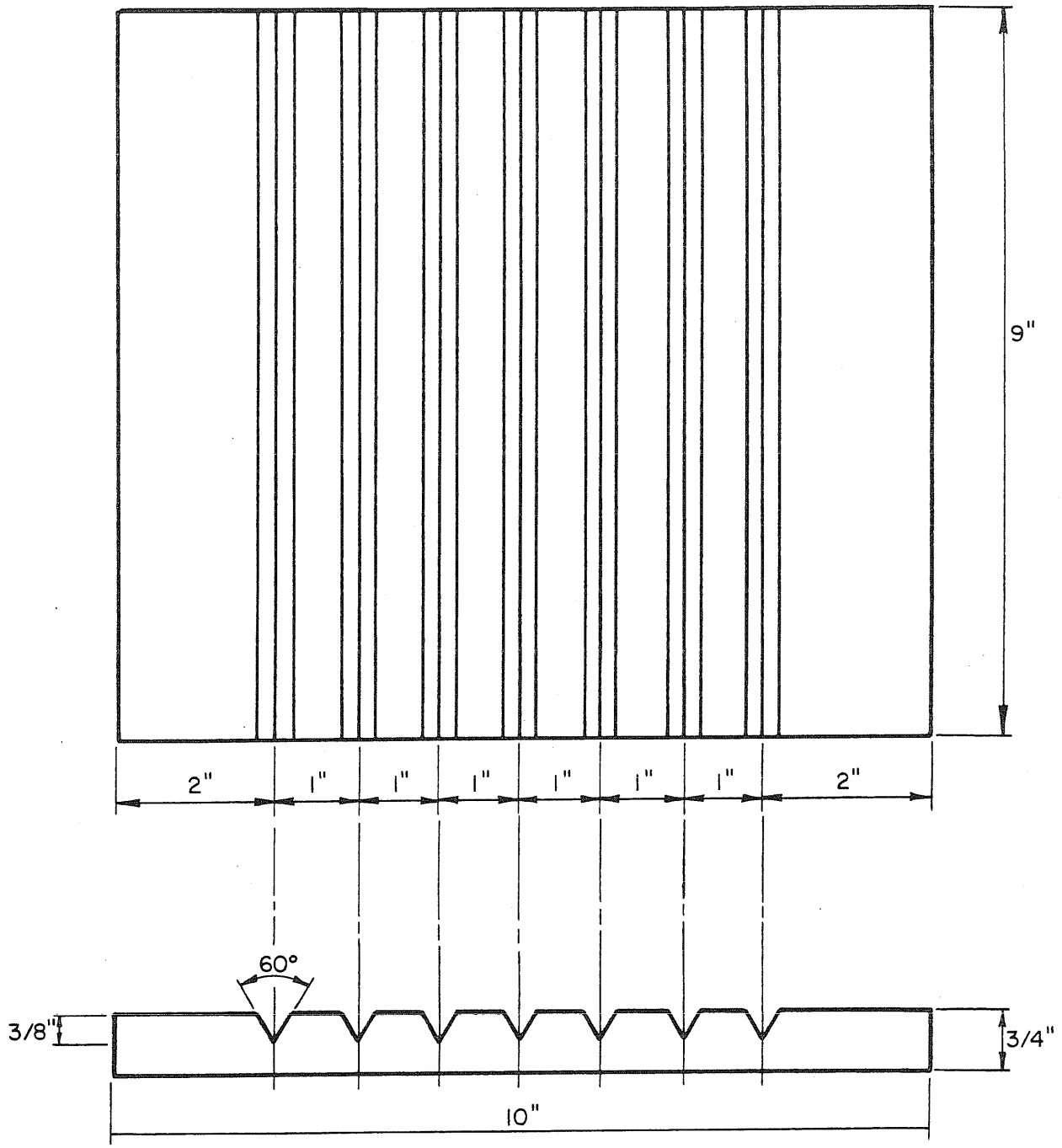

FIG. A.1 SKETCH OF V-GROOVE SAMPLE WELD PLATES

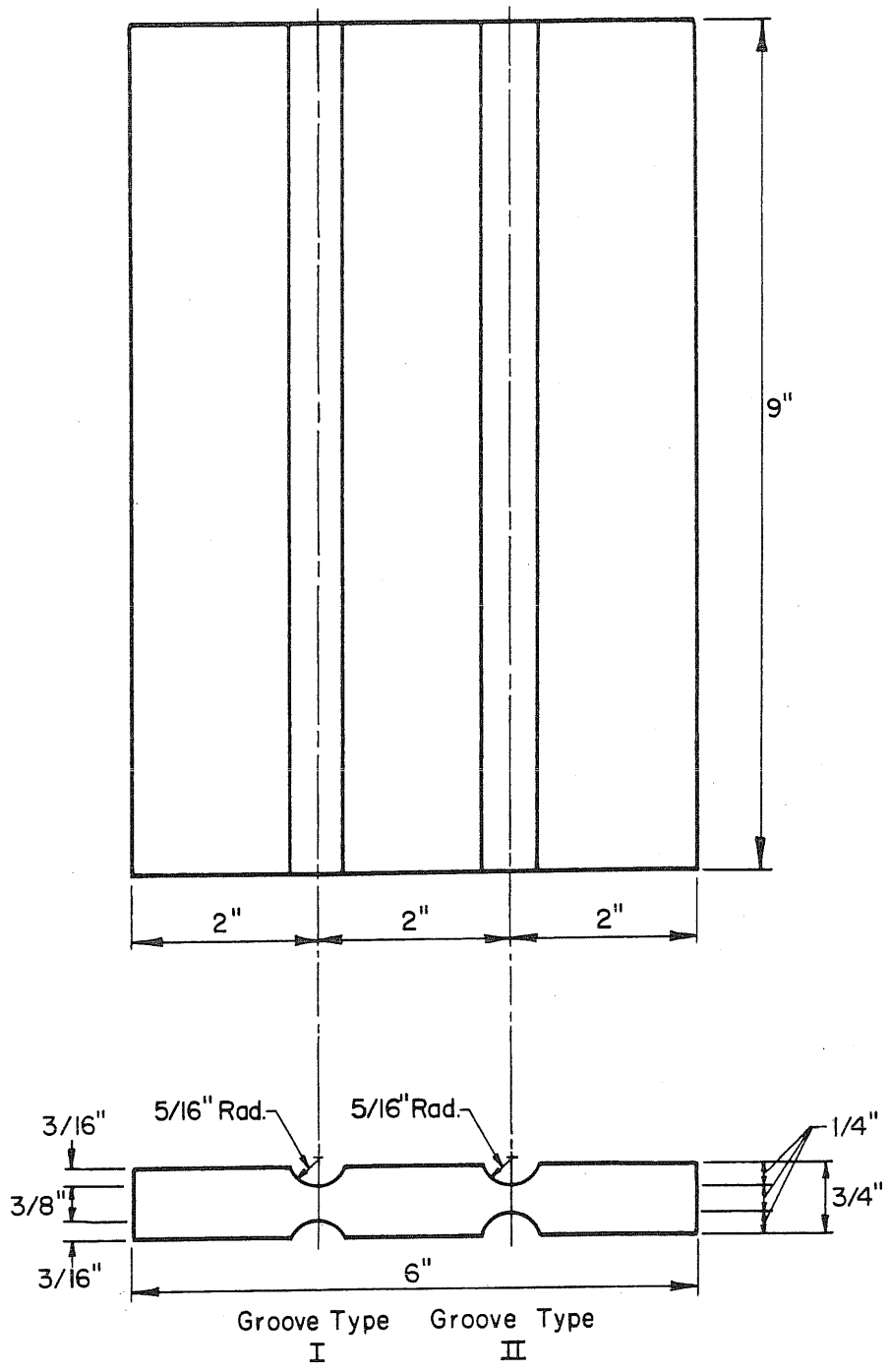

FIG. A.2 SKETCH OF U-GROOVE SAMPLE WELD PLATES

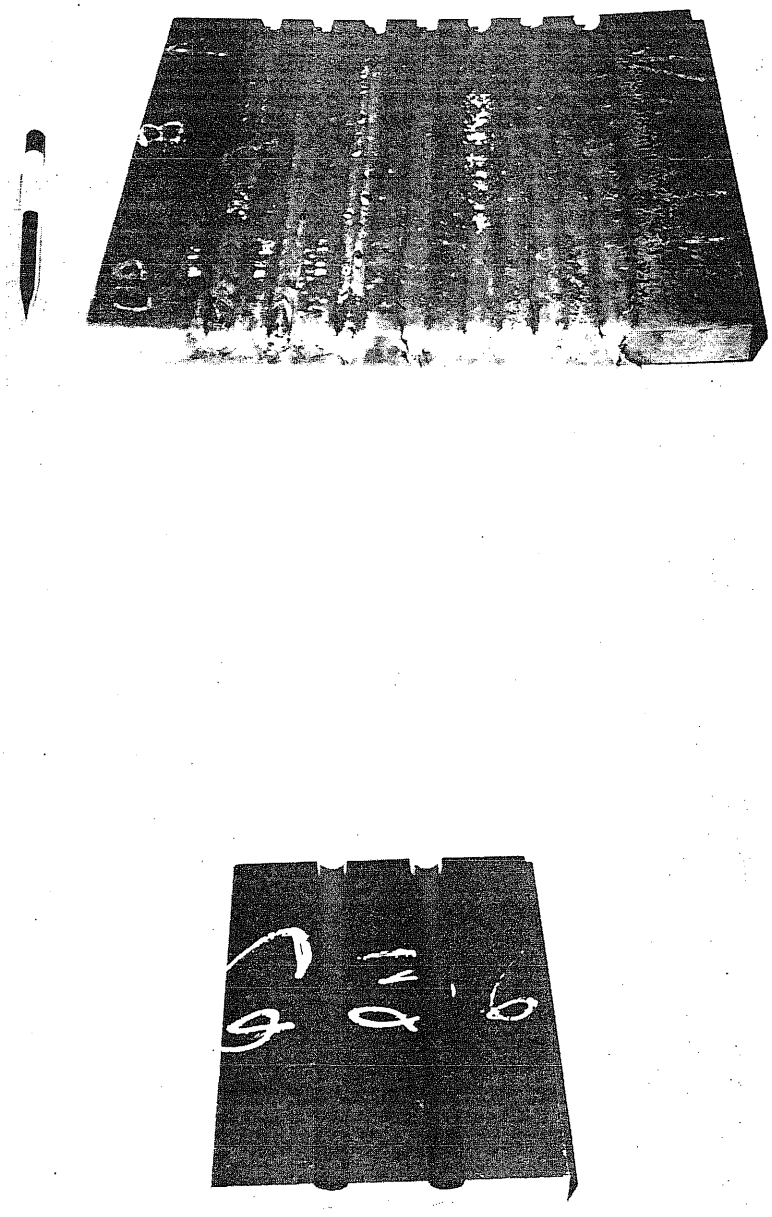

FIG. A.3 PHOTOGRAPH OF WELDED GROOVES IN WELD SAMPLE PLATE (a) V-GROOVES (b) U-GROOVES

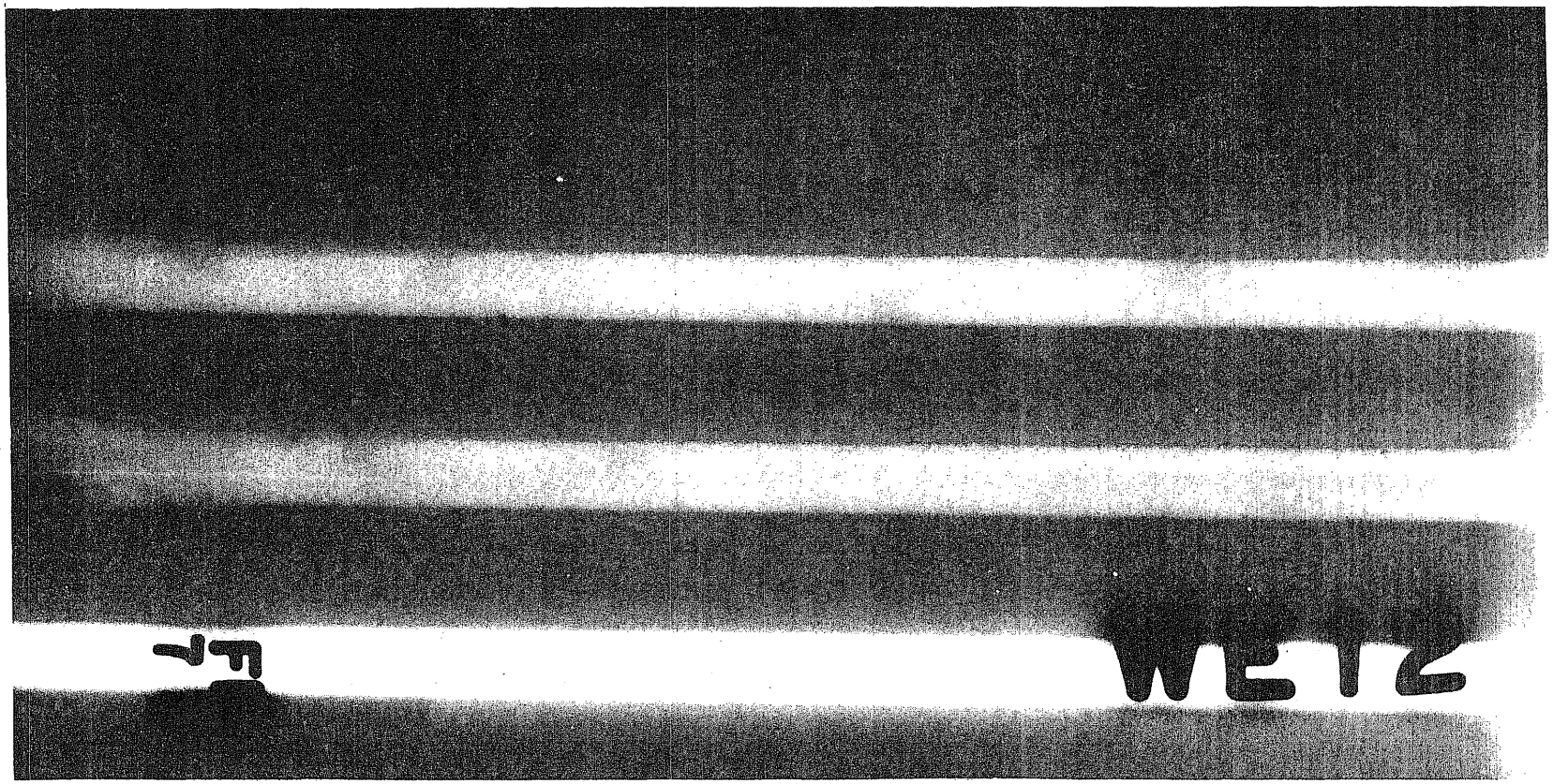

FIG. A.4 RADIOGRAPH OF SAMPLE WELDS FOR POROSITY AT CODE ALLOWABLE

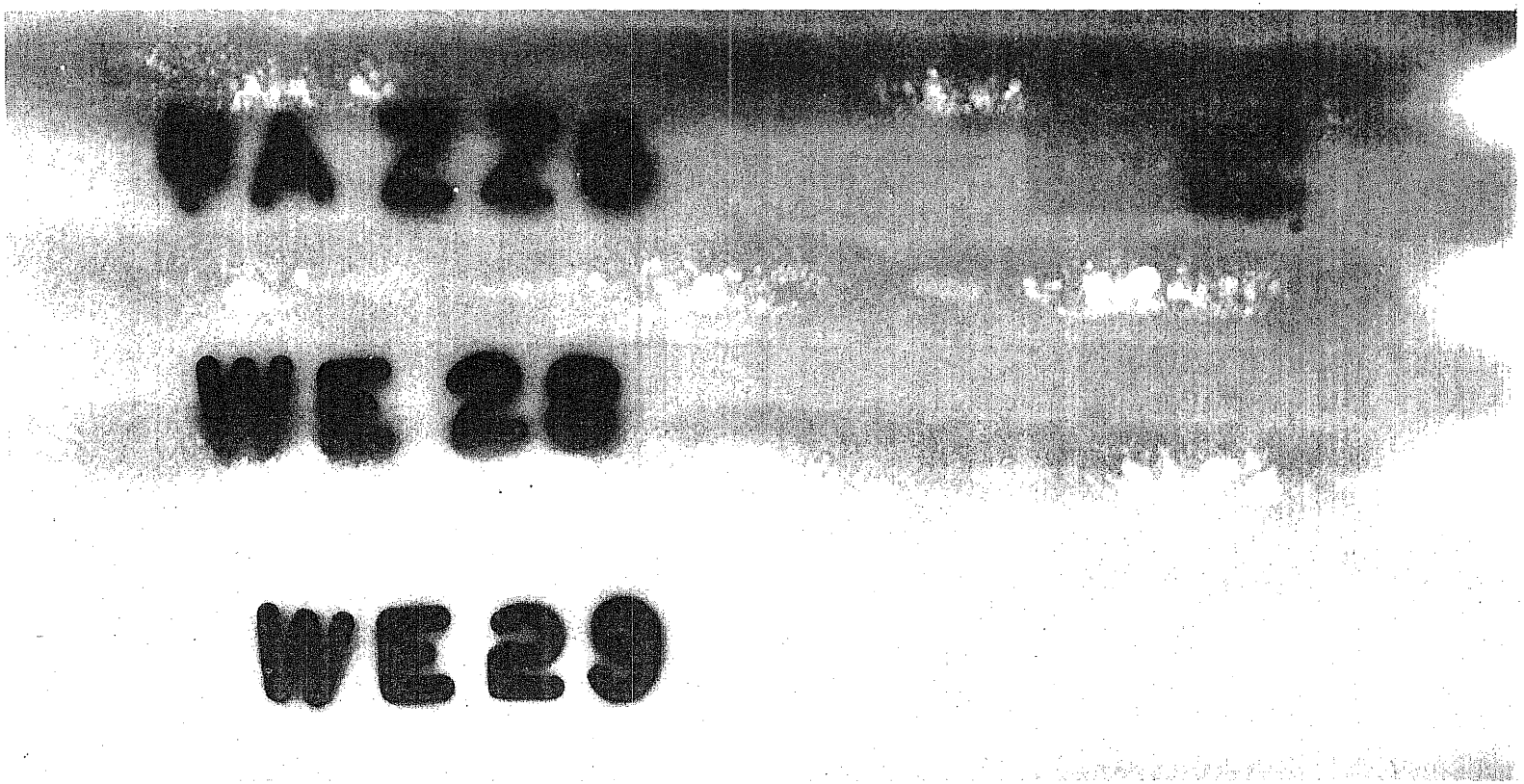

FIG. A.5 RADIOGRAPH OF SAMPLE WELDS FOR SEVERE POROSITY CLUSTERS

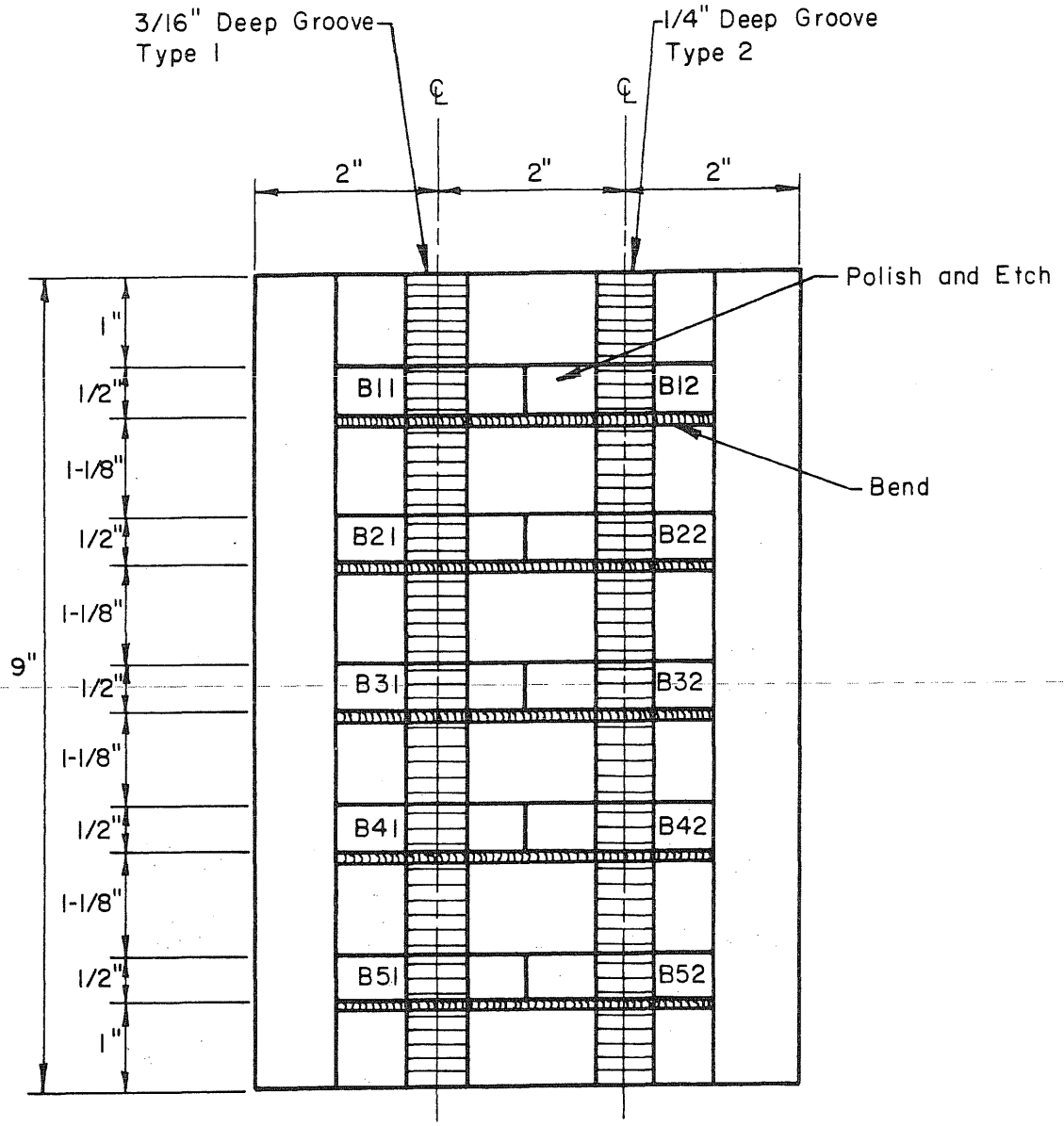

FIG. A.6 SPECIMENS FOR EXAMINATIONS OF LACK OF PENETRATION

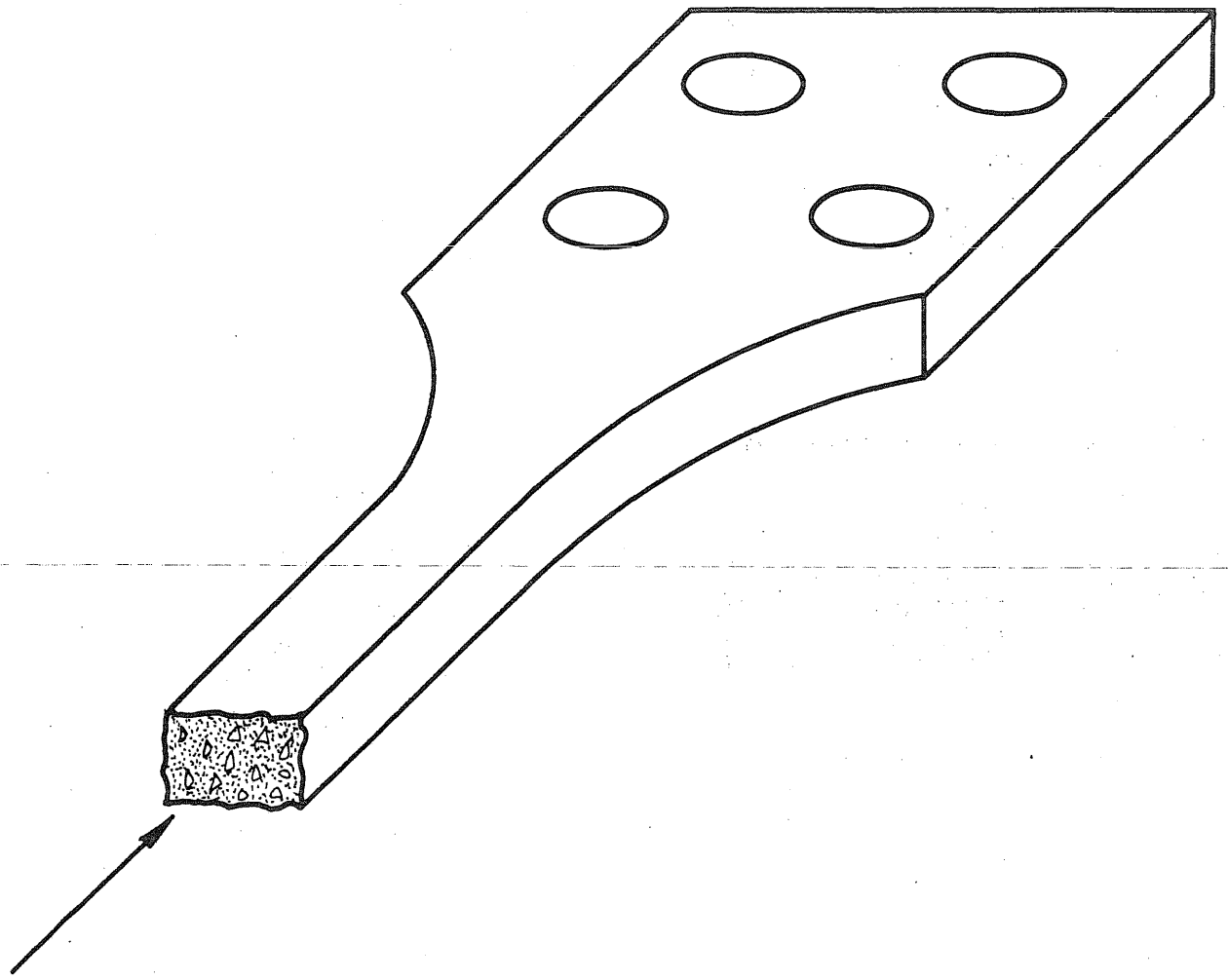

FIG. B.1 ORIENTATION OF FRACTURE SURFACE IN PHOTOGRAPHS OF FIGS. B.2 TO B.5

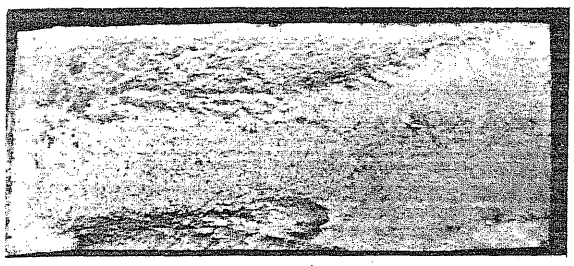

(a) SI-1B
Stress Range 43.7
Life-443,200

(b) SI-2
Stress Range 40.0
Life-630,800

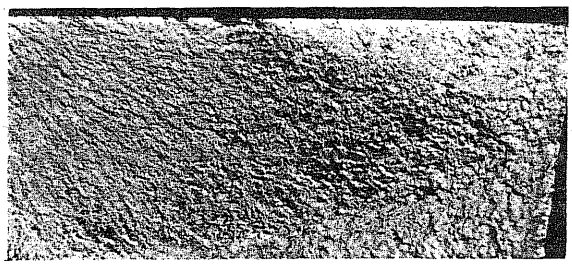

(c) SI-3A
Stress Range 46.0
Life-566,400

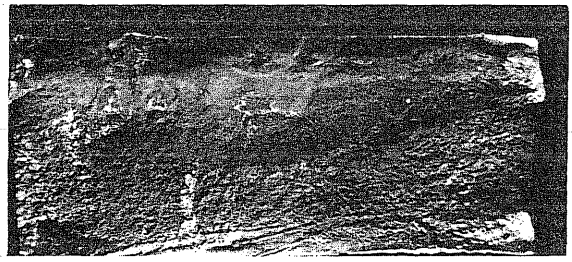

(d) SI-4
Stress Range 46.0
Life-262,700

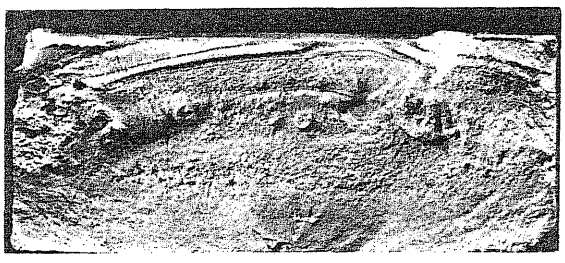

(e) SI-5
Stress Range 40.0
Life-2,691,800

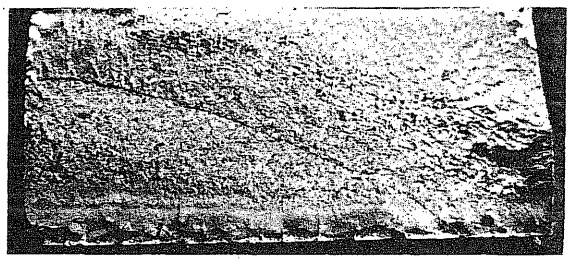

(f) LP2-3-1
Stress Range 46.0
Life-75,100

FIG. B.2 FRACTURE SURFACES OF SOUND WELDED JOINTS

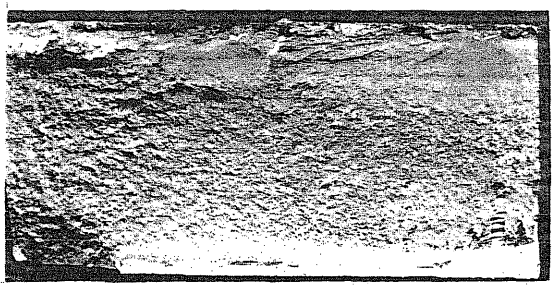

(g) LP2-3-2
Stress Range 46.0
Life-189,400

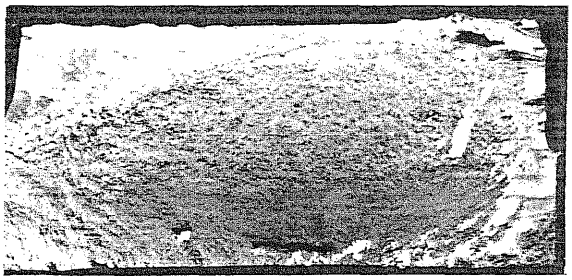

(h) LP2-3-3
Stress Range 46.0
Life-289,000

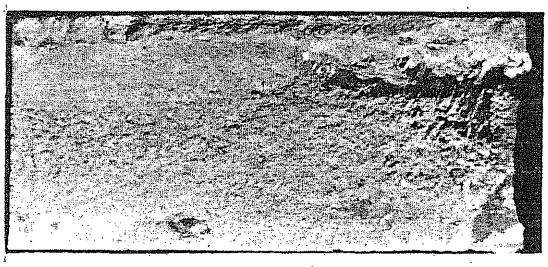

(i) LP 2-3-4
Stress Range 40.0
Life -275,700

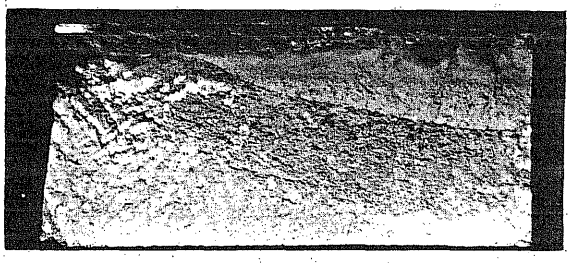

(j) LP2-3-5
Stress Range 51.0
Life-51,400

FIG. B.2 (cont.) FRACTURE SURFACES OF SOUND WELDED JOINTS

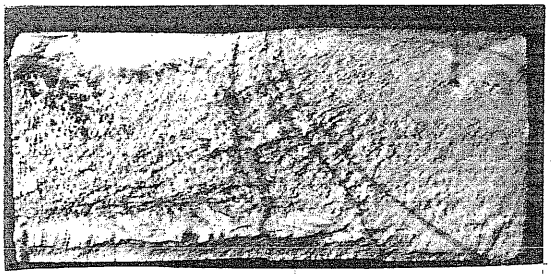

(a) PC 4-1
Stress Range 34.0
Life-1,485,500

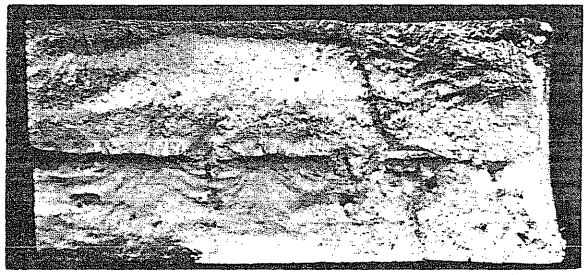

(b) PC 4-2
Stress Range 48.0
Life-5,353,800

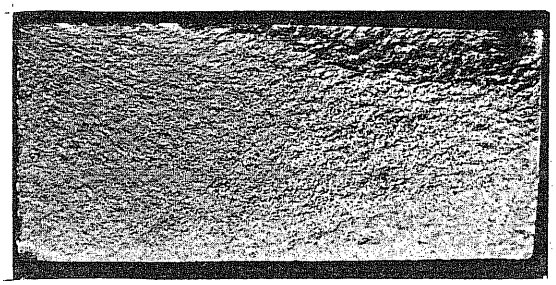

(c) PC 4 -3
Stress Range 56.0
Life-392,900

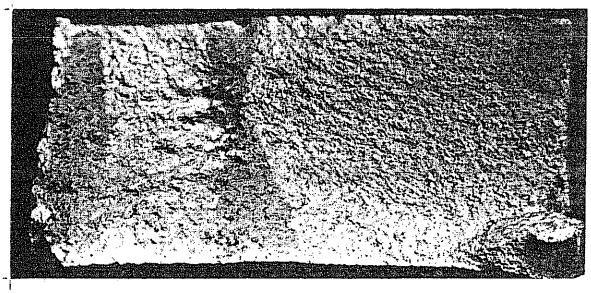

(d) PC 4-4
Stress Range 34.0
Life-107,100

FIG. B.3 FRACTURE SURFACES OF JOINTS WITH POROSITY AWS ALLOWABLE

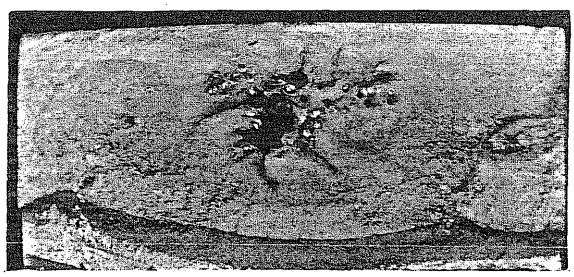

(a) PS 5-1
Stress Range 34.0
Life - 713,300

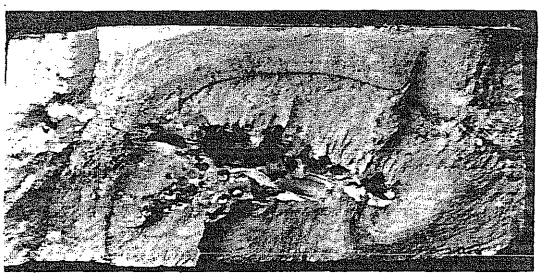

(b) PS 5-2
Stress Range 34.0
Life - 325,500

(c) PS 5-3
Stress Range 44.0
Life - 80,300

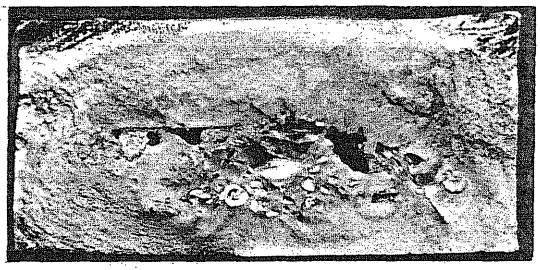

(d) PS 5-4
Stress Range 29.0
Life - 633,000

(e) PS 5-5
Stress Range 27.0
Life - 1,024,900

FIG. B.4 FRACTURE SURFACES OF JOINTS WITH SEVERE CLUSTERS OF POROSITY

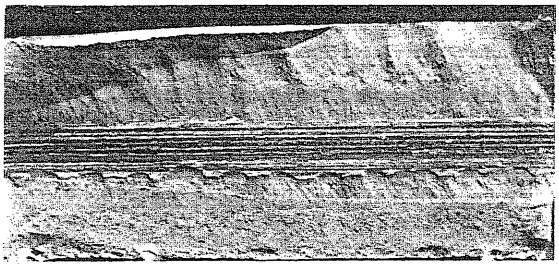

(a) LPI-2-1
Stress Range 34.0
Life-133,100

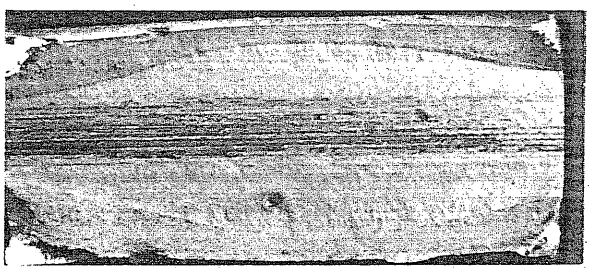

(b) LPI-2-2
Stress Range 20.0
Life-272,600

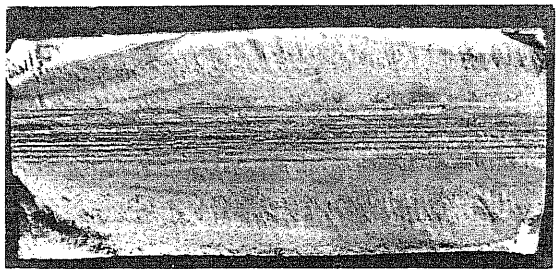

(c) LPI-2-3
Stress Range 16.9
Life-464,100

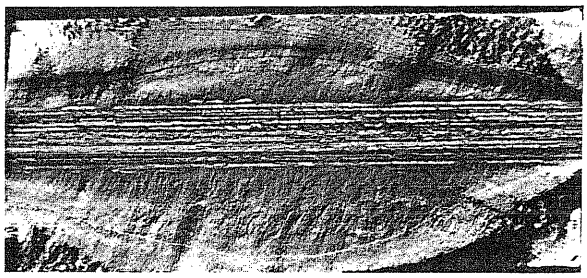

(d) LPI-2-4
Stress Range 34.0
Life-157,000

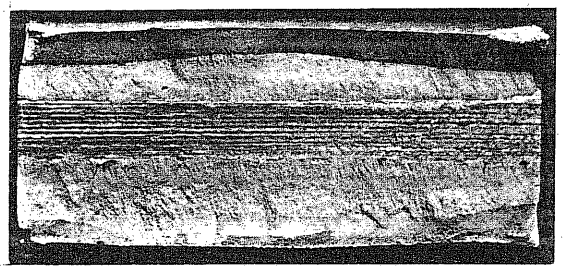

(e) LPI-2-5
Stress Range 34.0
Life-90,800

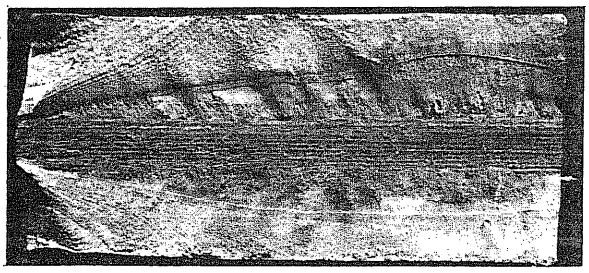

(f) LP 2-6-6
Stress Range 34.0
Life-50,200

FIG. B.5 FRACTURE SURFACES OF JOINTS WITH LACK OF PENETRATION

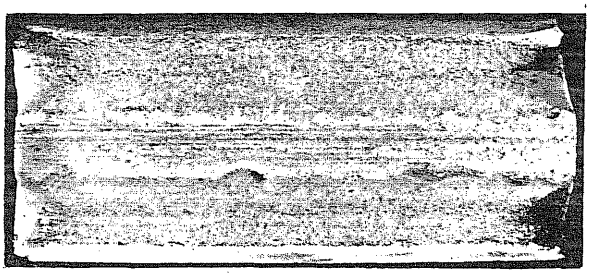

(g) LP2-6-7
Stress 68.6
Life-Static Test

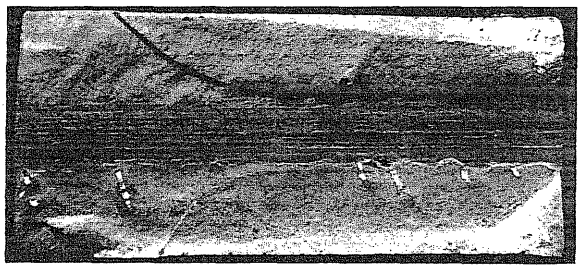

(h) LP2-6-8
Stress Range 22.0
Life-167,000

(i) LP2-6-9A
Stress Range 34.0
Life-469,900

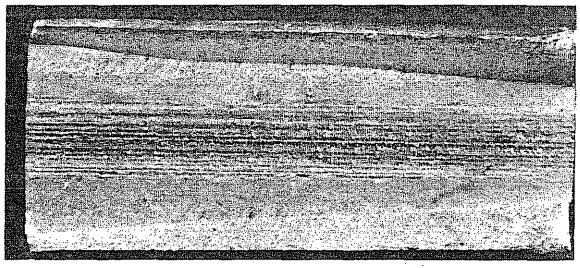

(j) LP2-6-10
Stress Range 15.0
Life-216,800

FIG. B.5 (cont.) FRACTURE SURFACES OF JOINTS WITH LACK OF PENETRATION

Appendix A--Preliminary Study of Welding Procedures

To study the effect of only one specific type and amount of defect in each specimen it was necessary to develop welding parameters to consistently reproduce the desired defects. However, before the parameters for defective welds could be determined, it was necessary to develop a procedure for sound welds and to qualify this procedure. The details of the welding procedure are presented in section 3.

The materials for the preliminary welding studies were the same as those used in the fabrication of the fatigue test specimens.

To examine the effects of the different parameters on weld porosity, trial welds were deposited in grooves cut in steel plates approximately 9-in. x 10-in. and 3/4-in. thick. The grooves were machined to half the plate thickness and with a 60° included angle, the same as the V-groove in the fatigue test specimens. Figure A.1 shows the details and dimensions of the plates. The sample plates for the study of lack of penetration were grooved with a U-groove similar to that to be used in the fatigue specimens. Initially, the groove was machined in a solid plate. However, to simulate more fully the actual fatigue specimen groove it was necessary to cut the plate, to machine the edges and tack weld the pieces together before machining the groove, just as for the fabrication of the fatigue test specimens (see Figure A.2).

Before qualifying the basic welding procedure it was necessary to select welding parameters that would produce a weld that contained no defects. To establish their soundness each of the welds was radiographed to determine whether defects were present. Each sample was welded with a

root pass and a cover pass. Two types of welding wire, different shielding gas mixtures, and various current and voltage settings were used to establish a set of parameters that could give radiographically sound welds. Qualification tests were then performed to verify the adequacy of the procedure selected. Next, having the welding parameters for a qualified sound weld, the changes necessary to produce the desired defects were established.

While examining the literature[5,7,8,9] on weld defects and welding by the gas-metal arc process, the following definitions of porosity and lack of penetration along with their common causes were identified. The list of causes indicate changes that might be made in the sound welding parameters to produce the desired defects.

Possible Methods for Controlling Weld Defects

1. Porosity--the formation of gas bubbles and their entrapment in the weld.

   Causes

   1. Excessive current and excessive arc length resulting in high consumption of deoxidizing elements when using gas shielded metal arc welding, resulting in porosity.
   2. Rapid cooling rates produce a uniform and fine porosity.
   3. Water vapor present in gas shields or on electrodes increases possibility and amount of porosity.
   4. Carbon dioxide shielded welds are highly oxidized. If the electrodes used are not suitably deoxidized (contain deoxidizing elements) porosity in the welds will form.

5. Excessively high voltage can cause spatter, undercut, and porosity at the edges of the weld.

6. Excessively low voltages cause porosity and overlap at the edges of the weld.

7. If joints are not clean it is possible that porosity in the weld could develop as a result.

8. The less oxygen present in the shielding gas the less stable the arc, resulting in considerable spatter and porosity.

2. Lack of penetration--failure of the materials to fuse integrally at the root of the weld. Frequently due to heat transfer conditions at the joint. If the arc does not cause the root to reach fusion temperature before some other point in the groove, the weld metal will be deposited across the root and screen the arc from it.

Causes

1. Root face dimension too great.

2. Root opening too small.

3. Included angle too small.

4. Use of too large an electrode.

5. High travel speed of weld placement (abnormal).

6. Insufficient welding current.

7. If the first pass is too slow the molten metal can get under the arc screening it from the root.

8. When using CO_2 shield negative electrodes give less penetration than positive electrodes.

9. Too high a voltage results in wider weld with less penetration.

The principal parameters that could be varied were the voltage, current, gas type, gas flow rate, travel speed and groove details. However, since it was desirable to be able to reproduce the selected defects

consistently, changes in voltage, gas type and gas flow were the most likely candidates to produce porosity, and the groove details could be altered to produce the lack of penetration. Table A.1 lists the variations that were introduced in the procedure to produce porosity type defects, the results of these modifications, and a comparison with the requirements of the AWS Specifications.[1] In some instances, some of the more difficult parameters to control were varied; these are presented in Table A.1 also. The procedure to produce a lack of penetration consisted simply of changing the groove detail from the V-groove to a U-groove and of varying the depth of the groove to the dimensions shown in Figure 3.2. The welding parameters were kept essentially unchanged from those of the sound weld procedure, the only difference being a slight change in the current.

To study the weld parameters two or three grooves were welded and then the quality of the weld determined radiographically before introducing any other variations in the parameters. If an attempt appeared successful (that is, if it produced the desired amount of defect) the same procedure was used several times to insure that the same defect could be reproduced consistently. In some of the grooves, as can be seen in Table A.1, a cover pass was welded over the defective pass to insure that it would not burn out the defects present in the initial pass (see Figures A.3, A.4 and A.5).

To determine the depth of penetration obtained in the lack of penetration samples, the sample plate was first radiographed to determine whether any other defects were present. Then it was cut into bend-test

strips and etch specimens as shown in Figure A.6. The width of the lack of penetration was then measured at each section to determine the uniformity of its dimension across the 9-in. width of plate. The polished and etched specimens and the bend strips are similar to those shown in Figure 3.8.

Although the desired amount of defect was obtained in a number of samples, the greatest consistency was obtained with the welding procedures that were finally chosen to fabricate the fatigue specimens. The procedures selected to produce the flaws desired in the welds are presented in section 3.

One other conclusion that can be drawn from this preliminary study of welding procedures is that although it is not difficult to produce a weld containing small defects which would meet the specification requirements, it is very difficult to produce severely defective welds without changing something drastically in the welding procedure.

Table A.1

WELDING VARIABLES STUDIED

Weld Sample No.	Pre-heat Temp. °F	Inter-pass Temp. °F	Gas Mix. %A-%O	Gas Flow CFH	Travel Speed IPM	Osc.*	Amps	Volts	AWS Spec.**	Remarks
WE1	150	150	98-2	50	12	No	325	27	Pass	Root Pass
							300	27		Pass No. 2
WE2	150	150	98-2	50	12	No	300	27	Fail	Both Passes
WE3	150	150	95-5	50	12	No	230	25	Pass	Root Pass
							250	28		Pass No. 2
WE4	150	150	95-5	50	12	No	280	28	Pass	Root Pass
							270	28		Pass No. 2
WQ1	150	150	95-5	50	12	No	280	28	Pass	Root Pass
							320	28		Pass No. 2
							310	28		Pass No. 3
							310	28		Pass No. 4
							280	28		Pass No. 5
							280	28		Pass No. 6
WE5	150	--	95-5	50	12	No	320	29		5" length
							320	30		5" length
WE6	150	--	95-5	50	12	No	320	27		2" length
							320	26		2" length
							320	25		2" length
							320	24		2" length
							320	23		2" length
WE7	150	--	95-5	50	12	No	320	25	Fail	One pass
WE8	150	--	95-5	50	12	No	320	26	Fail	One pass
WQ2	150	150	95-5	50	12	No	280	28	Pass	Root Pass
							320	28		Pass No. 2
							310	28		Pass No. 3
							310	28		Pass No. 4
							280	28		Pass No. 5
							280	28		Pass No. 6
WQ3	150	150	95-5	50	12	Yes	320	28	Pass	Root Pass
							330	28		Pass No. 2
							320	28		Passes 3-6

Table A.1 (Cont.)

Weld Sample No.	Pre-heat Temp. °F	Inter-pass Temp. °F	Gas Mix. %A-%O	Gas Flow CFH	Travel Speed IPM	Osc.*	Amps	Volts	AWS Spec.**	Remarks
WE9	150	--	95-5	50	12	No	320	25	Pass	One pass
WE10	150	--	95-5	50	12	No	320	26	Pass	One pass
WE11	150	--	95-5	50	12	Yes	330	25	Fail	One pass
WE12	150	--	95-5	50	12	Yes	330	26	Fail	One pass
WE13	150	--	95-5	50	12	Yes	330	25	Pass	One pass
WE14	150	--	95-5	50	12	Yes	330	26	Pass	One pass
WE15	150	--	95-5	25	12	Yes	330	28 26	Fail	5" length 5" length
WE16	150	--	95-5	5	12	Yes	330	28 26	Fail	5" length 5" length
WE17	150	--	95-5	15	12	Yes	330	28 26	Fail	5" length 5" length
WE18	150	--	95-5	15	12	Yes	330	28 26	Fail	5" length 5" length
WE19	150	--	95-5	50	12	Yes	330	28	Pass	Rust placed in weld
WE20	150	--	95-5	15	12	Yes	330	28/26		Periodic voltage reduction
WE21	150	--	95-5	15	12	Yes	330	28/26		Periodic voltage reduction
WE22	150	-- 150	95-5 95-5	50 50	50 12	Yes Yes	375 330	28 28		Root Pass Cover Pass
WE23	150	 150	98-2 98-2	20 20	12 12	Yes Yes	300 330	28/23 28		Root Pass Cover Pass
WE24	150	 150	98-2 98-2	20 50	12 12	Yes Yes	330 310	28/23 28		Root Pass Cover Pass
WE25	150	 150	98-2 98-2	20 50	12 12	Yes Yes	310/350 310	27 28		Root Pass Cover Pass

Table A.1 (Cont.)

Weld Sample No.	Pre-heat Temp. °F	Inter-pass Temp. °F	Gas Mix. %A-%O	Gas Flow CFH	Travel Speed IPM	Osc.*	Amps	Volts	AWS Spec.**	Remarks
WE26	150		98-2	50	12	Yes	310-350	28		Root Pass
		150	98-2	50	12	Yes	310	28		Cover Pass
WE27	150		95-5	50/0	12	Yes	330	28		Root Pass
		150	95-5	50	12	Yes	330	28		Cover Pass
WE28	150		95-5	50/0	12	Yes	320	28		Root Pass
		150	95-5	50	12	Yes	320	28		Cover Pass
WE29	150		95-5	50/0	12	Yes	330	28		Root Pass
		150	95-5	50	12	Yes	320	28		Cover Pass
WE30	150		100A	50	12	Yes	330-350	28,27,25		Root Pass
		150	95-5	50	12	Yes	330	28		Cover Pass
WE32	150		95-5	50	12	Yes	330	28		Water in groove
		150	95-5	50	12	Yes	330	28		Cover Pass
WE33	150		95-5	50	12	Yes	330	28		Oil in groove
		150	95-5	50	12	Yes	330	28		Cover Pass
WE34	150		95-5	50/0	12	Yes	330	28		Pinched hose @ 2", 4-1/2", and 7"
		150	95-5	50	12	Yes	330	28		Cover Pass
WE35	150		100A	50	12	Yes	250-350	28		Root Pass
		150	95-5	50	12	Yes	330	28		Cover Pass
WE36	150		100A	50	12	Yes	330-350	28		Root Pass
		150	95-5	50	12	Yes	330	28		Cover Pass
WE37	150		100A	50	12	Yes	400	28		Root Pass
		150	95-5	50	12	Yes	330	28		Cover Pass
WE38	150		95-5	50	12	Yes	330	25		Root Pass
		150	95-5	50	12	Yes	320	28		Cover Pass
WE39	150		95-5	50	12	Yes	330	25		Root Pass
		150	95-5	50	12	Yes	320	28		Cover Pass

Table A.1 (Cont.)

Weld Sample No.	Pre-heat Temp. °F	Inter-pass Temp. °F	Gas Mix. %A-%O	Gas Flow CFH	Travel Speed IPM	Osc.*	Amps	Volts	AWS Spec.**	Remarks
WE40	150		100A	50	12	Yes	330	25		Root Pass
		150	95-5	50	12	Yes	320	28		Cover Pass
WE41	150		100A	50	12	Yes	330	25		Root Pass
		150	95-5	50	12	Yes	320	28		Cover Pass

* Oscillator refers to whether the oscillator attached to welder as described in section 3 was used.

** AWS Specification[1]--This column indicates whether the weld passes the specification requirements or not.

NOTE: On some of the initial trial welds the groove was welded as machined. However, after noticing a line of incomplete penetration the groove was back-ground to better duplicate the condition of a back-ground first pass. It was necessary to place the defect in the second pass so it would be approximately at midthickness of the specimen and would not be ground out as the first pass was background.

Appendix B--Fracture Surfaces

All fatigue fractures were photographed in the direction shown in Figure B.1. The photographs in Figures B.2 to B.5 show the fracture surfaces, the stress at which the specimens were tested and the fatigue life. Further details of the tests are presented in Table 5.2. Specimens S1-1, S1-3, and LP2-6-9 did not fail at the original stress cycle. However, the stress was increased on these specimens and the test continued to failure. The fracture of these specimens are shown in Figures B.2(a), B.2(c) and B.5(i) respectively and the stress cycle and life shown are those used in the last portion of the testing. Specimen S1-3A in Figure B.2(c) broke in the base metal, as did specimens PC4-3 and PC4-4 shown in Figures B.3(c) and (d). Figure B.5(g) shows the fracture surface of specimen LP2-6-7 which was broken statically; it had not failed in the fatigue tests. These photographs clearly show the location and appearance of the defects in each of the specimens.

References

1. American Welding Society, *Specifications for Welded Highway and Railway Bridges*, AWS D2.0-69.
2. American Association of State Highway Officials, *Standard Specifications for Highway Bridges*, Tenth Edition, 1969 and 1971 Interim Specifications.
3. M. Hempel and H. Möller, "The Effect of Weld Defects in Specimens of Steel ST37 on Their Tensile Fatigue Strength," *Archiv für das Eisenhüttenwessen*, XX, No. 11 and 12, 1949.
4. R. P. Newman and M. G. Dawes, "Exploratory Fatigue Tests on Transverse Butt Welds Containing Lack of Penetration," British Welding Research Association, Report D2/6/62, August 1963.
5. W. M. Wilson, W. H. Munse, and I. S. Snyder, "Fatigue Strength of Various Types of Butt Welds Connecting Steel Plates," *Engineering Experiment Station Bulletin No. 384*, University of Illinois, March 1950.
6. H. Ottsen and W. H. Munse, "Three Dimensional Photoelastic Investigation of Simulated Weld Discontinuities," *Structural Research Series No. 358*, Civil Engineering Studies, University of Illinois, March 1970.
7. *Operator's Handbook, Trouble-Shooting Gas Metal-Arc Welding Processes and Equipment*, Miller Electric Manufacturing Company, Appleton, Wisconsin, 1967.
8. "How To Do--Manual Metal Inert Gas Welding," *Pamphlet F-51-110A*, Linde Division, Union Carbide Corporation.

9. American Welding Society, *Welding Handbook*, Sections 1 and 2, Sixth Edition, 1968.

10. F. V. Lawrence, Jr. and J. B. Radziminski, "Fatigue Crack Initiation and Propagation in High-Yield-Strength Steel Weld Metal," *Welding Journal*, Vol. 49, No. 10, October 1970.

11. T. Yokobori, M. Nanbu and N. Takeuchi, "Observation of Initiation and Propagation of Fatigue Crack by Plastic-Replication Method," Reports of the Research Institute for Strength and Fracture of Materials, Tohoku University, Sendai, Japan, Vol. 5, No. 1, November 1969.

12. T. Yokobori, "A Kinetic Theory of Fatigue Crack Propagation," Reports of the Research Institute for Strength and Fracture of Materials, Tohoku University, Sendai, Japan, Vol. 5, No. 1, November 1969.

13. J. D. Harrison, "The Analysis of Fatigue Test Results for Butt Welds with Lack of Penetration Defects Using a Fracture Mechanics Approach," *Welding Research Abroad*, Vol. XVII, No. 3, March 1971.

14. T. W. Crooker and E. A. Lange, "How Field Strength and Fracture Toughness Considerations Can Influence Fatigue Design Procedures for Structural Steels," *Welding Journal*, Vol. 49, No. 10, October 1970.

15. V. M. Barsom, E. J. Imhof, Jr., and S. T. Rolfe, "Fatigue Crack Propagation in High Strength Steels," U. S. Steel Tech. Report No. 39.018-007(27), December 20, 1968.

16. J. M. Barsom, "Review and Analysis of Fatigue-Crack-Propagation Laws," U. S. Steel Tech. Report No. 89.018-020(5), June 30, 1969.

17. F. Erdogan, "Crack Propagation Theories," *Fracture*, Vol. 2, 1968, (H. Liebowitz, ed.).